B6: Condensed Matter Physics

Toby Adkins

June 19, 2017

Contents

1. *An Introduction to Condensed Matter*

This chapter shall serve as an introduction to condensed matter physics, including a treatment of:

- Bonding Types
- Heat Capacity of Solids
- Electrons in Metals

Condensed matter physics deals with the macroscopic and microscopic properties of matter. In particular, is the concerned with the study of condensed phases that appear whenever the number of constituents in a system is very large, and interactions between the constituents are quite strong. We shall begin our study of this vast subject area by examining some of the consequences of studying condensed matter without a consideration of the periodic microscopic structure of the material. It shall be assumed that all readers are familiar with basic Statistical Mechanics.

1.1 Bonding Types

A sensible place to start our treatment of condensed matter would be to examine bonding, which is a word that is loosely used to describe mechanisms through which matter is held together. This shall give us some insight into the kinds of techniques that we will be required to use in a treatment of condensed matter more generally.

Below is a table that summarises the various properties of each of the bonding types that we will be considering, as it is useful to have a summary of much of the relevant information somewhere. It is recommended that students write out this table at least once in order to become familiar with its contents.

Bonding Type	Description	Typical Atoms	Typical Properties
Ionic	An electron is transferred from one atom to another, and the resulting ions attract one another	Binary compounds made of constituents with very different electro-negativity, such as Group I and VII	• Hard, very brittle • High melting temperature • Electrical insulators • Water soluble
Covalent	An electron is shared equally between two atoms, forming a bond. The energy of the electron is lowered by the delocalisation of the wavefunction	Solids of only one element (diamond), or compounds of similar electro-negativities, such as Group III and V	• Very hard • High melting temperature • Electrical Insulators or semiconductors
Metallic bonds	Electrons are delocalised throughout the solid, acting as a bonding agent between the ions	Metals, found on the left and in the middle of the Periodic Table	• Ductile and malleable due to the non-directional nature of the bond • Lower melting temperature • Good electrical and thermal conductors
Molecular (Van-der-Waals or Fluctuating Dipole)	There is no transfer of electrons. The dipole moments of the constituents align, causing attraction between themselves. Bonding strength increases with the size of the molecules and their polarity	Noble gas solids, or solids made of slightly polar molecules binding together	• Soft and weak • Low melting temperature • Electrical insulators
Hydrogen	Involves an H^+ ion bound to one atom, but still attracted to another	Important in organic and biological materials	• Weak bond (stronger than molecular however) • Important for maintaining the shape of DNA and proteins

Table 1.1: A summary of bonding types

1.1.1 Ionic Bonding

In *ionic bonds*, an electron is transferred from one atom to another, and the resulting ions attract one another. As we know, the ionisation energy is the energy cost to ionise one of the atoms in order to liberate the electron. Then, the *electron affinity* is the energy increase for an atom when it gains an electron and become a negatively charged ion. Lastly, the *cohesive energy* is the energy released upon the formation of the bond, as the delocalisation of the electron between the two atoms decreases the overall energy associated with its spatial wavefunction. In order for a bond to form, we require the total energy released in the formation of the bond to be positive. That is, we require that

$$\Delta E = \text{Electron Affinity} + \text{Cohesive Energy} - \text{Ionisation Energy} \tag{1.1}$$

Both the electron affinity and ionisation energy must be determined empirically for various substances, but we can approximate the cohesive energy by the Coulomb repulsion term between the two nuclei

$$\text{Cohensive Energy} \approx \frac{e^2}{4\pi\epsilon_0 R} \tag{1.2}$$

where R is the internuclear separation. One often finds that the value of ΔE predicted by (1.1) is actually more than that which is observed experimentally. This is due to the fact that in writing (1.2), we have assumed that the two ions behave as charged point-particles. This approximation evidently breaks down as the atoms are brought together, as we have to take into account the complicated interaction of the electron clouds of the two nuclei. As such, the potential energy is no longer an r^{-1} curve, but instead diverges as $r \to 0$, which raises the energy of the system for a given molecular separation.

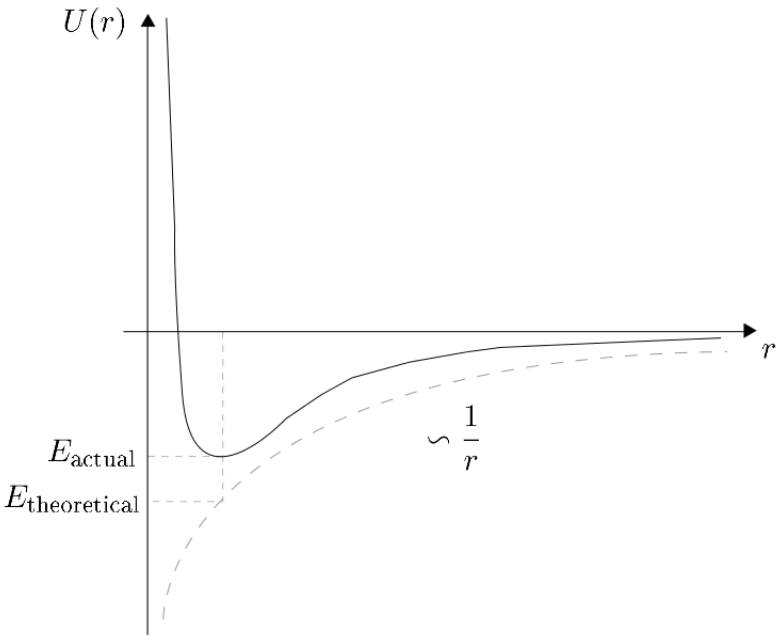

Figure 1.1: A comparison between the real and theoretical potential energy curves for ionic bonding

1.1.2 Covalent Bonding

We can get a handle on covalent bonding using the *tight-binding model*, a model that we will revisit later in chapter 3.2.2 when we have dealt with periodic structures. Let us consider a single electron that is sitting in the potential of two identical positive nuclei.

Making the Born-Oppenheimer approximation (see B3 notes for more information on this), we can write the Hamiltonian of the electron as

$$H = T + V_1 + V_2, \quad T = \frac{\mathbf{p}^2}{2m_e}, \quad V_i = \frac{e^2}{4\pi\epsilon_0 |\mathbf{r} - \mathbf{R}_i|} \tag{1.3}$$

where $\mathbf{R}_i$ are the (fixed) positions of the nuclei and $\mathbf{r}$ is the position of the electron. Such a system a system satisfies the Time-Independent Schrödinger Equation

$$H|\psi\rangle = E|\psi\rangle, \quad |\psi\rangle = \sum_n \phi_n |n\rangle \tag{1.4}$$

where we have assumed that the overall state $|\psi\rangle$ can be written as a superposition of eigenstates $|n\rangle$. This means that

$$\sum_n H\phi_n |n\rangle = \sum_n E\phi_n |n\rangle \quad \longrightarrow \quad \sum_n \langle m| H |n\rangle \phi_n = \sum_n E\phi_n \langle m|n\rangle \tag{1.5}$$

Defining the *Hamiltonian matrix* $H_{nm} = \langle n| H |m\rangle$, *orthogonality matrix* $O_{nm} = \langle n|m\rangle$, and letting $\boldsymbol{\phi} = (\phi_1, \ldots, \phi_n)$, we can write an effective Schrödinger equation

$$\boxed{(O^{-1}H)\boldsymbol{\phi} = E\boldsymbol{\phi}} \tag{1.6}$$

which we can solve for the eigenvalues and eigenstates of the system. This is often known as the *linear-combination of atomic orbitals (LCAO)*. Note that for orthogonal eigenstates, the orthogonality matrix simply becomes the identity matrix.

For covalent bonding, let us consider a state of the form

$$|\psi\rangle = \phi_1 |1\rangle + \phi_2 |2\rangle \tag{1.7}$$

where $|1\rangle$ and $|2\rangle$ correspond to the electron being localised to the first and second nuclei respectively. We then make the approximation that these states are orthogonal, which will evidently break down as the nuclei are brought closer together. Then, we can write our Hamiltonian matrix as

$$H = \begin{pmatrix} \langle 1| H |1\rangle & \langle 1| H |2\rangle \\ \langle 2| H |1\rangle & \langle 2| H |2\rangle \end{pmatrix} = \begin{pmatrix} E_0 + V_c & -t \\ -t^* & E_0 + V_c \end{pmatrix} \tag{1.8}$$

where we have defined the matrix elements

$$H_{11} = \langle 1| T + V_1 |1\rangle + \langle 1| V_2 |1\rangle = E_0 + V_c \tag{1.9}$$

$$H_{22} = \langle 2| T + V_2 |2\rangle + \langle 2| V_1 |2\rangle = E_0 + V_c \tag{1.10}$$

$$H_{12} = H_{21}^* = \langle 1| T + V_2 |2\rangle + \langle 1| V_1 |2\rangle = -t \tag{1.11}$$

E_0 is simply the hydrogenic energy of the electron when associated with a single nucleus. V_c is the *cross-term* energy associated with the fact that an electron in orbital $|1\rangle$ feels an Coulomb attraction with the second nucleus, or vice-versa (as the system has exchange symmetry). The term $-t$ is known as the *hopping term* that is the energy associated with the electron moving between the two orbitals. This can be simply solved for the eigenvalues and eigenstates:

$$E_\pm = E_0 + V_c \pm |t|, \quad \psi_+ = \frac{1}{\sqrt{2}}(\phi_1 + \phi_2), \quad \psi_- = \frac{1}{\sqrt{2}}(\phi_1 - \phi_2) \tag{1.12}$$

These are symmetric and antisymmetric wavefunctions (similar to the groundstate and first excited state of a particle in a box), corresponding to a greater and smaller spatial

separation of the nuclei respectively. However, we can argue that the V_c should cancel the repulsion between the nuclei. Consider a surface S_1 surrounding the electron 'cloud' of the first nucleus. By Gauss' law, the field outside S_1 is zero. This means that so long as the second nucleus is outside the electron cloud of the first nucleus, the repulsion felt by the nuclei will cancel with V_c to first order. Thus, as we have initially neglected nuclear repulsion in our consideration of the energy levels, these become

$$E_{\pm} \approx E_0 \pm |t| \tag{1.13}$$

Thus means that - for the lower eigenstate at least - it can be energetically favourable to form such a bond. This argument must break down when the atoms get sufficiently close to one another, as the Gauss' law argument will no longer hold, meaning that V_c will not cancel the repulsion, as well as the fact that we will no longer be able to consider orthogonal states.

1.1.3 Molecular Bonding

Van-der-Waals bonding arises due to the tendency of electric dipoles to align and attract one another. Suppose that we have two atoms separated by a distance $r = |\mathbf{r}|$, where the first has a dipole moment $\mathbf{p}_1$. Then, the second feels an electric field of

$$\mathbf{E} = \frac{|\mathbf{p}_1|^2}{4\pi\epsilon_0}\frac{\hat{\mathbf{r}}}{r^3} \tag{1.14}$$

Assuming that it is polarisable, the second atom will develop a dipole moment according to $\mathbf{p}_2 = \chi_e \mathbf{E}$ due to this field. The potential energy that is associated with the interaction between these two dipoles is then given by

$$U(r) = -\mathbf{p}_2 \cdot \mathbf{E} = -\frac{|\mathbf{p}_1|^2 \chi_e}{(4\pi\epsilon_0)^2}\frac{1}{r^6} \tag{1.15}$$

This means that we have an attractive force $\mathbf{F} = -\nabla U \propto r^{-7}$, that quickly drops off with separation. It is thus a very weak form of bonding. Note that this argument appears to depend on the fact that the dipole moment of $\mathbf{p}_1$ of the first atom is non-zero, despite the fact that on average it will be zero. However, we are saved by that fact that (1.15) is a function of $|\mathbf{p}_1|^2$, which has a non-zero expectation value.

1.1.4 Thermal Expansion

Thermal expansion is the tendency of matter to change in shape, area and volume in response to a change in temperature. Here, we shall consider the thermal expansion of a two-atom solid, and then qualitatively generalise this result to more complicated systems. From statistical mechanics, the expectation value for the extension is given by

$$\boxed{\langle x \rangle = \frac{\int dx\, x e^{-\beta V(x)}}{\int dx\, e^{-\beta V(x)}}} \tag{1.16}$$

where as usual $\beta = (k_B T)^{-1}$, and $V(x)$ is some potential between the two atoms. Assuming sufficiently small energies, we can expand this potential as

$$V(x) \approx \underbrace{\frac{\kappa_2}{2!}(x - x_0)^2}_{\text{harmonic term}} - \underbrace{\frac{\kappa_3}{3!}(x - x_0)^3}_{\text{anharmonic term}} + \dots \tag{1.17}$$

where we have defined the energy at the minimum of the potential to be zero. Now, assuming that the contribution from the anharmonic term is much smaller than the thermal energy $\kappa_3 \langle x \rangle^3 \ll k_B T$, we can expand the exponential term in (1.16) as

$$e^{-\beta V(x)} \approx e^{-\frac{\beta\kappa_2}{2}(x-x_0)^2}\left[1 + \frac{\beta\kappa_3}{3!}(x-x_0)^3 + \dots\right] \tag{1.18}$$

and extend the limits of the integration to $[-\infty, \infty]$. This is because the integration of these terms over this infinite domain will still only create a small contribution to the overall energy when compared with the dominant thermal energy. We can then approximate the *coefficient of thermal expansiveness* α as being given by

$$\alpha = \frac{1}{L}\frac{dL}{dT} = \frac{1}{x_0}\frac{d\langle x \rangle}{dT} \tag{1.19}$$

Performing the integration, we find that this is given explicitly by

$$\alpha = \frac{1}{x_0}\frac{k_B\kappa_3}{2\kappa_2^2} \tag{1.20}$$

Now, this result assumes fixed, periodic potential wells, which could at first glance easily be generalised to higher dimensions. While this remains a good approximation, there are extra degrees of freedom (such as lattice vibrations - more on these later) that will disrupt the fixed nature of these potentials in higher dimensions, meaning that more refined techniques are required.

We shall note here the definition of compressibility (or elasticity) for future reference:

$$\beta_s = -\frac{1}{V}\frac{\partial V}{\partial p} \approx -\frac{1}{L}\frac{\partial L}{\partial F} \tag{1.21}$$

where the second approximation follows from considering a one-dimensional system of length L subject to some compressive force F.

1.2 Heat Capacity of Solids

Now that we have at least a shallow understanding of bonding, let us have a look at another property of solids that is often examined, that of *heat capacity*. In general, this is defined as

$$\boxed{C_{(\dots)} = \left(\frac{\partial U}{\partial T}\right)_{(\dots)}} \tag{1.22}$$

where $(\dots)$ stands for the quantity that is held constant, such as temperature T, pressure p or volume V. Of course, we already know what this is in the high-temperature limit due to the *equipartition theorem*:

> *If the energy of a classical system is the sum of q quadratic modes, and the system is in contact with a heat reservoir at temperature T, then the mean energy of the system is given by $U = \frac{1}{2}qk_BT$.*

This means that the heat capacity of classical solids consisting of N atoms is given roughly by $C = 3Nk_B = 3R$, where R is the universal gas constant. This is sometimes known as *The Law of Dulong-Petit*, and appears to hold very well at room temperatures, though for lower temperatures, all materials start to deviate from this prediction. We shall seek to model this deviation over the course of this section.

1.2.1 Classical Oscillator

The logical place to begin is with a classical description of solids, which will also serve as a reminder of the basics manipulations associated with Statistical Mechanics. In this model, we treat each of the N atoms within a sample as a classical harmonic oscillator sitting within its three-dimensional potential, such that each can be described by the Hamiltonian

$$H(\mathbf{p}, \mathbf{x}) = \frac{\mathbf{p}^2}{2m} + \frac{1}{2!}k\mathbf{x}^2 \tag{1.23}$$

for some spring constant $k = m\omega^2$. The associated single particle partition function is then given by

$$Z_1 = \frac{1}{(2\pi\hbar)^3}\int d^3\mathbf{p}\int d^3\mathbf{x}\, e^{-\beta H(\mathbf{p},\mathbf{x})} = \frac{1}{(2\pi\hbar)^3}\left(\int_{-\infty}^{\infty} dp_x\, e^{-\frac{\beta}{2m}p_x^2}\right)^3\left(\int_{-\infty}^{\infty} dx\, e^{-\frac{\beta k}{2}x^2}\right)^3 \tag{1.24}$$

Note that the normalisation factor ensures that the partition function is indeed dimensionless. Evaluating these integrals using

$$\int_{-\infty}^{\infty} dx\, e^{-ax^2+bx} = e^{b^2/4a}\sqrt{\frac{\pi}{a}} \tag{1.25}$$

we find that

$$Z_1 = \frac{1}{(\beta\hbar\omega)^3}, \quad \omega = \sqrt{\frac{k}{m}} \tag{1.26}$$

Then, the internal energy is given clearly by

$$U \equiv -\frac{\partial \log Z_1}{\partial \beta} = 3k_BT \tag{1.27}$$

For N independent atoms, $Z = Z_1^N$, such that the internal energy becomes $U = 3Nk_BT$. We thus recover the Law of Dulong-Petit when we calculate the heat capacity.

Anharmonic Terms

A more interesting case to consider is where there are anharmonic terms entering into our potential. Due to the symmetry of the problem, these can only be even powers of x. Thus, the first order perturbation on (1.23) is given by

$$H = \frac{\mathbf{p}^2}{2m} + \frac{1}{2!}k\mathbf{x}^2 + \frac{1}{4!}\lambda\mathbf{x}^4 \tag{1.28}$$

for some small parameter λ. As before, the single particle partition function is

$$Z_1^\lambda = \frac{1}{(2\pi\hbar)^3}\int d^3\mathbf{p}\, e^{-\frac{\beta}{2m}\mathbf{p}^2}\int d^3\mathbf{x}\, e^{-\frac{\beta k}{2}\mathbf{x}^2-\frac{\beta\lambda}{4!}\mathbf{x}^4} \tag{1.29}$$

We can solve this by using the series expansion for the exponential, and differentiating under the integral:

$$\begin{aligned}\int d^3\mathbf{x}\, e^{-\frac{\beta k}{2}\mathbf{x}^2-\frac{\beta\lambda}{4!}\mathbf{x}^4} &= \int d^3\mathbf{x}\sum_n \frac{1}{n!}\left(\frac{\beta\lambda}{4!}\mathbf{x}^4\right)^n e^{-\frac{\beta k}{2}\mathbf{x}^2}\\ &= \sum_n \frac{1}{n!}\left(-\frac{\beta\lambda}{4!}\left[\frac{2}{\beta}\frac{\partial}{\partial k}\right]^2\right)^n \int d^3\mathbf{x}\, e^{-\frac{\beta k}{2}\mathbf{x}^2}\\ &= \exp\left(-\frac{\beta\lambda}{4!}\frac{4}{\beta^2}\frac{\partial^2}{\partial k^2}\right)\int d^3\mathbf{x}\, e^{-\frac{\beta k}{2}\mathbf{x}^2}\end{aligned} \tag{1.30}$$

This means that we can write that

$$Z_1^\lambda = \exp\left(-\frac{\beta\lambda}{4!}\frac{4}{\beta^2}\frac{\partial^2}{\partial k^2}\right)Z_1 \tag{1.31}$$

where Z_1 is as in the harmonic case (1.26). To first order, we can expand this as

$$Z_1^\lambda = \left(1-\frac{\lambda}{6\beta}\frac{\partial^2}{\partial k^2}\right)Z_1 = \frac{1}{(\beta\hbar\omega)^3}\left(1-\frac{5\lambda}{8k^2}\frac{1}{\beta}\right) \tag{1.32}$$

The heat capacity is given by

$$C_V = \frac{\partial}{\partial T}\left(-\frac{\partial}{\partial\beta}\log Z_1^\lambda\right) = \frac{\beta}{T}\frac{\partial^2\log Z_1^\lambda}{\partial\beta^2} = 3k_B - \frac{5}{4}\frac{\lambda}{m^2\omega^4}k_BT \tag{1.33}$$

where we have made use of the fact that $\partial/\partial T = -(\beta/T)\partial/\partial\beta$, and assumed the classical limit such that $\beta \ll 1$. Note that this result is well-behaved in the limit that $\lambda \to 0$. What is of interest to us is that it predicts a temperature dependence for the heat capacity when the potential is not strictly harmonic.

1.2.2 Einstein Model

Similarly to above, the Einstein model treats each of these atoms as individual quantum harmonic oscillators. For a one-dimensional quantum harmonic oscillator, the energy levels are given by

$$E_n = \left(n+\frac{1}{2}\right)\hbar\omega \tag{1.34}$$

for some oscillator frequency ω. Then, the single particle partition function is

$$Z_1 = \sum_{n=0}^{\infty} e^{-\beta\hbar\omega\left(n+\frac{1}{2}\right)} = e^{-\frac{1}{2}\beta\hbar\omega}\sum_{n=0}^{\infty}e^{-\beta\hbar\omega} = \frac{e^{-\frac{1}{2}\beta\hbar\omega}}{1-e^{-\beta\hbar\omega}} \tag{1.35}$$

For a three-dimensional solid consisting of N individual atoms, the entire partition function can be written as $Z = {Z_1}^{3N}$, such that

$$\boxed{Z = \left[2\sinh\left(\frac{1}{2}\beta\hbar\omega\right)\right]^{-3N}} \tag{1.36}$$

The internal energy follows simply from this

$$U = -\frac{\partial \log Z}{\partial \beta} = \frac{3}{2}N\hbar\omega\coth\left(\frac{1}{2}\beta\hbar\omega\right) \tag{1.37}$$

We can also write this as

$$U = 3N\hbar\omega\left(\bar{n}_i + \frac{1}{2}\right), \quad \bar{n}_i = \frac{g_i}{e^{\beta(E_i-\mu)}-1} \quad \text{for} \quad \begin{cases} E_i = \hbar\omega \\ g_i = 1 \\ \mu = 0 \end{cases} \tag{1.38}$$

where n_i are the individual occupation numbers given by Bose-Einstein statistics. This means that each potential well looks like a system of bosons, as we can fill up the states indefinitely. The heat capacity can then be found trivially as

$$\boxed{C_V = 3Nk_B(\beta\hbar\omega)^2\frac{e^{\beta\hbar\omega}}{\left(e^{\beta\hbar\omega}-1\right)^2}} \tag{1.39}$$

Let us examine the limits of this expression:

- Low temperatures: $\beta\hbar\omega \gg 1$, $e^{\beta\hbar\omega} \gg 1$, such that

$$C_V = 3Nk_B(\beta\hbar\omega)^2 e^{-\beta\hbar\omega} \tag{1.40}$$

- High temperatures: $\beta\hbar\omega \ll 1$, $e^{\beta\hbar\omega} \approx 1 + \beta\hbar\omega$, such that

$$C_V = 3Nk_B \tag{1.41}$$

The Einstein model thus clearly recovers the law of Dulong-Petit at high temperatures, and also the 'freeze-out' of the vibrational modes when energy is insufficient to excite them at low temperatures. However, this model does not encapsulate the whole picture; it predicts that the heat capacity decreases exponentially at low temperatures, where as in actuality, we observe a power-law dependence.

1.2.3 Debye Model

The Debye model of heat capacity treats the vibrations of the lattice due to thermal excitations as *phonons*; discrete quanta of vibration, essentially a 'quantised wave'. If we think of a phonon as being a particle (analogously to a photon for light waves), then it is clear that phonons can occupy the same states, meaning that they must obey Bose-Einstein statistics

$$\bar{n}_i = \frac{1}{e^{\beta\hbar\omega_i}-1} \tag{1.42}$$

where we have again set $\mu = 0$. We then assume that

1. Phonons obey the dispersion relation $\omega = c_s k$, where c_s is the speed of sound in the given material

2. There are three modes of polarisation (1 longitudinal, 2 transverse) in three-dimensions, rather than two

3. The wavenumber of the phonons cannot be larger than the inverse spacing of atoms in the lattice. This limits the degrees of freedom, giving rise to a maximal frequency

$$\hbar\omega_D = k_B T_D \tag{1.43}$$

where ω_D and T_D are the Debye temperature and frequency respectively

With these assumptions in mind, let us calculate the density of states for these phonons:

$$g(k)d^3\mathbf{k} = \underbrace{3}_{\text{number of modes}} \frac{V}{(2\pi)^3} 4\pi k^2 dk = \frac{3V}{2\pi^2} k^2 dk \tag{1.44}$$

where we have assumed that our crystal is isotropic in k space. Using the dispersion relation from above, this density of states can be written in terms of frequency

$$g(\omega)d\omega = \frac{3V}{2\pi^2 c_s^3}\omega^2 d\omega \tag{1.45}$$

Suppose that we have N atoms within our material. In order for there to be $3N$ degrees of freedom - in agreement with the classical limit - we must define the Debye frequency, such that

$$\int_0^{\omega_D} d\omega\, g(\omega) = 3N \quad \longrightarrow \quad \omega_D = c_s(6n\pi^2)^{1/3} \tag{1.46}$$

This allows us to re-write our density of states as

$$g(\omega)d\omega = 9N\left(\frac{\hbar}{k_B T_D}\right)^3 \omega^2 d\omega \tag{1.47}$$

where we have used the definition of T_D (1.43). Recalling (1.42), the internal energy of the system can then be written as

$$U = \int d\omega\, \bar{n}_i g(\omega)\hbar\omega = 9N\hbar\left(\frac{\hbar}{k_B T_D}\right)^3 \int_0^{\omega_D} d\omega\, \frac{\omega^3}{e^{\beta\hbar\omega} - 1} \tag{1.48}$$

As is usual for these sorts of expressions, we non-dimensionalise the integrand using the substitution $x = \beta\hbar\omega$:

$$\boxed{U = 9Nk_B T\left(\frac{T}{T_D}\right)^3 \int_0^{T_D/T} dx\, \frac{x^3}{e^x - 1}} \tag{1.49}$$

We can now examine the heat capacity predicted by this model in two asymptotic limits:

- Low temperatures: $T \ll T_D$, $T_D/T \to \infty$, such that

$$U = 9Nk_B T\left(\frac{T}{T_D}\right)^3 \underbrace{\int_0^{\infty} dx\, \frac{x^3}{e^x - 1}}_{\pi^4/15} = \frac{3}{5}\pi^4 Nk_B T\left(\frac{T}{T_D}\right)^3 \tag{1.50}$$

meaning that our expression for the heat capacity becomes

$$C_V = 3Nk_B\,\frac{4}{5}\pi^4\left(\frac{T}{T_D}\right)^3 \tag{1.51}$$

This means that at very low temperatures, the Debye theory predicts a cubic dependence on temperature

- High temperatures: $T_D \ll T$, $e^x \approx 1 + x$ over the region of integration, such that

$$U = 9Nk_BT\left(\frac{T}{T_D}\right)^3 \int_0^{T/T_D} dx\, x^2 = 3Nk_BT \tag{1.52}$$

  which clearly recovers the law of Dulong-Petit as we require

The Debye theory works well in the extreme temperature limits, but is only approximate for intermediate temperatures. Another cause for alarm is the fact that the phonons obey the sound dispersion relation $\omega = c_s k$ for all values of k, where-as sound waves are generally only defined for long wavelengths, and thus small k. Furthermore, it does not take into account the linear dependence on temperature in the heat capacity for metals at low temperatures, something that we shall take care of in the next section.

1.3 Electrons in Metals

Thus far, there has been very little consideration of the behaviour of electrons within the solids that we are considering. For most solids, it is fine to ignore the electrons, as they will remain tightly bound to atoms and will not introduce further degrees of freedom into the system. However, this is not the case in metals, as the electrons are delocalised throughout the material, and thus can contribute to macroscopic properties of the material. We shall consider two theories of electrons in metals, neither of which make an explicit reference to the periodic microscopic structure of the given metal, which in itself limits both theories.

1.3.1 Drude Theory

Drude theory involves the kinetic treatment of electrons in metals, neglecting any electromagnetic interactions between electrons, or any exclusion effects. This theory is based on three main assumptions:

1. The electrons have a mean time τ between collisions. The probability of a scattering occurring within a time dt is $P = dt/\tau$
2. Once a scattering event occurs, the electron has some fraction of its original momentum $\lambda\mathbf{p}$, $0 < \lambda < 1$. Note that this is usually given as the electron has momentum $\mathbf{p} = 0$ after the collision; we do not need to make this strong an assumption
3. In between scattering events, the electrons are subject to the Lorentz force $\mathbf{F} = -e(\mathbf{E} + \mathbf{v} \times \mathbf{B})$

The first two of these are similar to the assumptions made in kinetic theory, while the third takes into account the fact that the electrons are charged particles. Consider an electron with momentum $\mathbf{p}$ at a time t. Then, its momentum at a time $t + dt$ is given by

$$\langle \mathbf{p}(t + dt) \rangle = P \langle \mathbf{p} \text{ after scattering} \rangle + \bar{P} \langle \mathbf{p} \text{ after no scattering} \rangle \tag{1.53}$$

where P is the probability of scattering as above, and $\bar{P} = 1 - P$ is the probability of not scattering. Writing $\langle \mathbf{p} \rangle \equiv \mathbf{p}$, this becomes

$$\mathbf{p}(t + dt) = \left(1 - \frac{dt}{\tau}\right)(\mathbf{p}(t) + \mathbf{F}dt) + \frac{dt}{\tau}\lambda\mathbf{p} \quad \longrightarrow \quad \frac{d\mathbf{p}}{dt} = \mathbf{F} - \mathbf{p}\left(\frac{1}{\tau}(1 - \lambda)\right) \tag{1.54}$$

This means that we can simply re-define our definition of the collision timescale, such that we can write

$$\boxed{\frac{d\mathbf{p}}{dt} = -e(\mathbf{E} + \mathbf{v} \times \mathbf{B}) - \frac{\mathbf{p}}{\tau}} \tag{1.55}$$

where we have written the Lorentz force explicitly. This is our evolution equation for the expectation value of the momentum of the electrons within our metal.

Conductivity and Resistivity

We can solve this in the steady state, recalling that $\mathbf{p} = m\mathbf{v}$ and $\mathbf{j} = -ne\mathbf{v}$:

$$0 = -e\mathbf{E} + \frac{\mathbf{j} \times \mathbf{B}}{n} + \frac{m}{ne\tau}\mathbf{j} \quad \longrightarrow \quad \mathbf{E} = \frac{1}{ne}\mathbf{j} \times \mathbf{B} + \frac{m}{ne^2\tau}\mathbf{j} \tag{1.56}$$

Define the *resistivity* ρ of a sample as the matrix satisfying $\mathbf{E} = \rho\mathbf{j}$; that is, it relates the electric field within a sample to the current density. By inspection of (1.56), this is clearly given by

$$\rho = \begin{pmatrix} 1/\sigma_0 & B_z/ne & -B_y/ne \\ -B_z/ne & 1/\sigma_0 & B_x/ne \\ B_y/ne & -B_x/ne & 1/\sigma_0 \end{pmatrix}, \quad \sigma_0 = \frac{ne^2\tau}{m} \tag{1.57}$$

Without loss of generality, we can consider the magnetic field to be orientated along $\mathbf{e}_z$. Then, using the method of cofactors, we can invert the matrix ρ to find the conductivity matrix $\sigma = \rho^{-1}$ as

$$\sigma = \frac{\sigma_0}{1+(\omega_c\tau)^2}\begin{pmatrix} 1 & -\omega_c\tau & 0 \\ \omega_c\tau & 1 & 0 \\ 0 & 0 & 1+(\omega_c\tau)^2 \end{pmatrix}, \quad \omega_c = \frac{e|\mathbf{B}|}{m} \tag{1.58}$$

where σ_0 is defined as above, and ω_c is the familiar *cyclotron frequency.*

The Hall Effect

The *Hall effect* is the production of a voltage or potential difference across a conductor when a magnetic field is applied in a direction perpendicular to the flow of current. An experimental set-up used to investigate this is shown in figure 1.2.

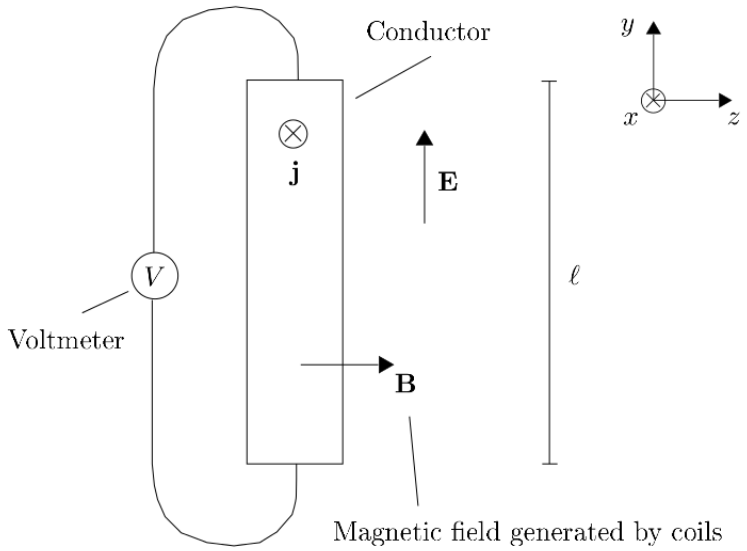

Figure 1.2: A schematic diagram of the experimental set-up used to investigate the Hall effect

We define the *Hall coefficient* R_H and *Hall voltage* V_H as

$$\boxed{R_H = \frac{\rho_{yx}}{|\mathbf{B}|} = -\frac{1}{ne}, \quad V_H = R_H\frac{I\,|\mathbf{B}|}{t}} \tag{1.59}$$

where t is the thickness of the sample in the direction parallel to the magnetic field. This means that by measuring the E_y that results from the application of j_x and B_z, the charge carrier density n can unlikely be determined from the Hall coefficient. However, this can often prove experimentally difficult for a number of reasons:

- Thermal fluctuations within the material may generate small EMF's, creating currents that effect the reading of the Hall voltage as its magnitude is comparable with the scale of these fluctuations
- The magnetic field needs to be calibrated properly to ensure that it is uniform throughout the sample
- The contact pins used to connect the voltmeter circuit to the conductor have a finite resistance, which provides an offset error in the data that needs to be accounted for

- The contact pins must be properly aligned, such that they are indeed measuring $E_y \ell$, instead of some perpendicular component of the voltage. This can be done through multiple measurements of moving one contact, which will cause the measured voltage to fluctuate around some value

Often, the Hall coefficient is measured experimentally to have the opposite sign to that expected from the above analysis. This indicates the presence of positive charge carriers that are not included in Drude theory. The nature of these charge carries will be revealed in section 3.3.

Thermal Transport

Recall the expression for the thermal conductivity of a kinetic gas:

$$\kappa = \frac{1}{3} n c_v \langle v \rangle \lambda \tag{1.60}$$

where c_v is the heat capacity per particle, $\langle v \rangle$ is some mean velocity, and $\lambda = \langle v \rangle \tau$ the mean-free path. Assuming that

$$c_v = \frac{3}{2} k_B, \quad \langle v \rangle = \frac{2}{\sqrt{\pi}} v_{th} = \left(\frac{8 k_B T}{\pi m} \right)^{1/2} \tag{1.61}$$

the thermal conductivity can be written as

$$\kappa = \frac{4}{\pi} \frac{n \tau k_B^2 T}{m} \tag{1.62}$$

While this quantity still has the unknown scattering timescale τ in it, it also occurs in the electrical conductivity σ_0 in (1.57). Thus, we often consider the ratio of the thermal conductivity to electrical conductivity, known as the *Lorenz number*:

$$L = \frac{\kappa}{\sigma_0 T} = \frac{4 k_B^2}{\pi e^2} \approx 0.94 \times 10^{-8} \text{ Watt Ohm K}^{-2} \tag{1.63}$$

This result appears to differ from experiment by only a factor of order unity. This is quite astounding that this theory should predict the correct order of magnitude considering that it is a purely kinetic theory. It turns out that this is due to the fact that we have hugely overestimated the heat capacity per electron, but hugely underestimated the typical velocities of electrons (see (1.73)); these two errors roughly cancel one another out.

1.3.2 Sommerfeld Theory

Sommerfeld theory treats the electrons within metals as a degenerate fermionic gas, such that the mean occupation numbers will behave according to

$$\bar{n}_i = \frac{1}{e^{\beta(E-\mu)} + 1} \to \begin{cases} 1 & \text{for } E < \mu(T=0) \\ 0 & \text{for } E > \mu(T=0) \end{cases} \tag{1.64}$$

This is shown in figure 1.3. This means that electrons will begin to 'stack up' and occupy all the available single particle states from the lowest to some maximum energy at $T = 0$. We thus define the *Fermi energy* as

$$E_F = \mu(T=0) \tag{1.65}$$

That is, the value of the chemical potential at $T = 0$, corresponding to the maximum energy per particle at this temperature. Let us find an expression for the Fermi energy.

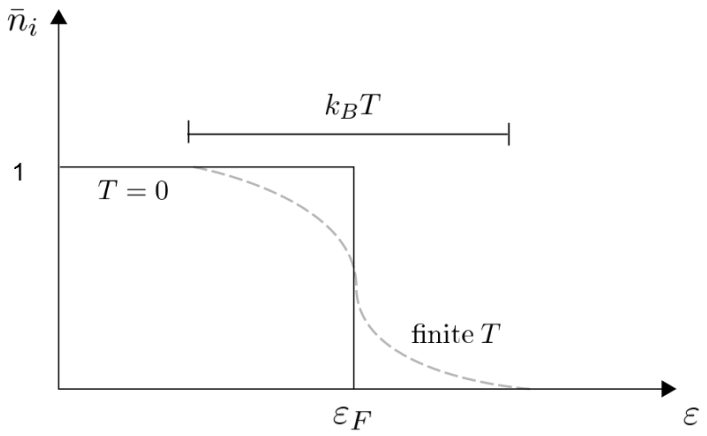

Figure 1.3: The occupation numbers for $T = 0$ and some finite correction

Assume that the electrons are non-relativistic, such that we can adopt the usual energy dispersion relation

$$E = \frac{p^2}{2m} = \frac{\hbar^2 k^2}{2m} \tag{1.66}$$

such that the density of states becomes

$$g(E)dE = \frac{(2s+1)Vm^{3/2}}{\sqrt{2}\pi^2\hbar^3}E^{1/2}dE = \frac{3N}{2E_F^{3/2}}E^{1/2} \tag{1.67}$$

Then, we can determine E_F as the analytic solution to some equation for N, the number of electrons within the system, remembering that $\bar{n}_i$ behaves as a step-function at absolute zero:

$$N = \sum_n \bar{n}_i = \int_0^{E_F} dE\, g(E) = \frac{(2s+1)Vm^{3/2}}{\sqrt{2}\pi^2\hbar^3}\,\frac{2}{3}E_F^{3/2} \tag{1.68}$$

Rearranging, we find that the Fermi energy is given by

$$\boxed{E_F = \left(\frac{6\pi^2 n}{2s+1}\right)^{2/3}\frac{\hbar^2}{2m}} \tag{1.69}$$

We can use this to find a criterion under which using Sommerfeld theory is valid. Looking at Figure (1.3), it is clear that whether we can approximate $\bar{n}_i$ as a step-function is limited by the width of the curve (k_BT) and so this treatment is valid for temperatures satisfying

$$T \ll T_F = \frac{E_F}{k_B} \backsim \frac{\hbar^2 n^{2/3}}{mk_B}$$

where T_F is known as the *Fermi temperature*. This can be interpreted as roughly the temperature at which the electron gas becomes degenerate. The condition is indeed satisfied in most metals at room temperature.

We can also define the *Fermi-wavevector*

$$k_F = (3\pi^2 n)^{1/2} \tag{1.70}$$

The surface of the sphere (in k space) of radius k_F is known as the *Fermi surface*, which divides the filled states from un-filled states at zero temperature. We will consider the Fermi surface in more detail later, but it is useful to introduce it here.

Mean Free Path

An informative exercise is to check whether our assumption that electrons within metals are free is indeed correct. By analogy to Drude theory, we can model the effect of the process of electrons scattering off ions as a relaxation equation for the Fermi surface

$$\frac{d\mathbf{k}}{dt} = -\frac{\mathbf{k}}{\tau} - \frac{e}{\hbar}\mathbf{E} \tag{1.71}$$

where τ is the collisional timescale. In the steady state, this becomes

$$\mathbf{k} = -\frac{e\tau}{\hbar}\mathbf{E} \tag{1.72}$$

such that the electron drift velocity is given by

$$\mathbf{v}_d = \frac{\hbar\mathbf{k}}{m} = -\frac{e\tau}{m}\mathbf{E} \tag{1.73}$$

Recalling the definition of the current density $\mathbf{j}$, we can find the conductivity σ in terms of the scattering time

$$\mathbf{j} = \sigma\mathbf{E} = -ne\mathbf{v}_d \quad \longrightarrow \quad \sigma = \frac{ne^2\tau}{m} \tag{1.74}$$

Now, τ is defined as the average time between the scattering collisions for an individual electron. Since the scattering processes only involve electrons in states close to E_F, the collisional timescale can be taken to be $\tau = \lambda/v_F$, where λ is the mean-free-path, and $v_F = \hbar k_F/m$ is the *Fermi velocity*. Thus, the mean-free-path becomes

$$\boxed{\lambda = \frac{m\sigma v_F}{ne^2}} \tag{1.75}$$

Comparing this to the typical spacing between atoms in metals $a \backsim n^{-1/3}$, it becomes clear that the mean-free-path is much greater than this value, meaning that we are able to apply Sommerfeld theory to metals.

Heat Capacity

As we increase the temperature above $T = 0$ in a degenerate Fermi gas, there is some excitation above E_F. For small corrections, the number of excited particles $\Delta N_{\text{exc.}}$ is given roughly by

$$\Delta N_{\text{exc.}} \backsim g(E_F)\Delta E \tag{1.76}$$

However, looking at figure 1.3, the width of the curve is roughly $\Delta E \backsim k_B T$. This means that the change in energy of the system due to the temperature increase scales as

$$\Delta U \backsim \Delta N_{\text{exc.}}\Delta E \backsim \frac{N}{E_F}(k_B T)^2 \tag{1.77}$$

Differentiating this expression, we can approximate the heat capacity of a degenerate Fermi gas by'

$$C_V = Nk_B\frac{k_B T}{E_F} \tag{1.78}$$

This equation is valid up to numerical constants of order unity (the constant is $\pi^2/2$ for those that are wondering). A more accurate result can be found by considering the Sommerfeld expansion of some arbitrary function $f(E)$ around $T = 0$:

$$\int_0^\infty dE\, \frac{f(E)}{e^{\beta(E-\mu)}+1} \approx \int_0^\mu dE\, f(E) + \frac{\pi^2}{6}f'(\mu)(k_B T)^2 + \dots \tag{1.79}$$

We shall no do this here however; being familiar with a scaling argument is enough.

We now have a much more accurate prediction of the heat capacity of metals at low temperatures, as we are able to write it as

$$\boxed{C_V = c_1 T + c_2 T^3} \tag{1.80}$$

The first term is the contribution from the electronic heat capacity as predicted by the Sommerfeld model, while the second is the contribution from the phononic heat capacity according to the Debye model. This relationship is observed experimentally.

Pauli Paramagnetism

The Fermi gas within metals is able to display *Pauli paramagnetism*, whereby free electrons tend to align their spins anti-parallel to an applied magnetic field, and thus inducing a magnetisation parallel to it. The Hamiltonian for a free electron within an applied magnetic field $\mathbf{B}$ is given by

$$H = \frac{\mathbf{p}^2}{2m_e} + g_s \frac{\mu_B}{\hbar} \mathbf{B} \cdot \mathbf{S} \tag{1.81}$$

Aligning $\mathbf{B}$ along $\mathbf{e}_z$, this has the associated energy levels of

$$E_\pm = \frac{\hbar^2 k^2}{2m_e} \pm \mu_B B \tag{1.82}$$

We do see that being spin-down relative to the direction of the magnetic field is energetically favourable, the reason behind the induced magnetisation. To find the magnetisation, we will make use of the grand potential Φ defined by

$$\Phi = F - \mu N = -k_B T \log \mathcal{Z}, \quad N = -\left(\frac{\partial \Phi}{\partial \mu}\right)_{T,V} \tag{1.83}$$

where $\mathcal{Z} = \sum_\alpha e^{-\beta(E_\alpha - \mu N_\alpha)}$ is the grand partition function. Suppose that Φ_0 is the grand potential in the absence of an applied magnetic field, and assume that the magnetic field is weak, such that $\mu_B B \ll E_F$. Then, it follows that

$$\Phi = \frac{1}{2}\Phi_0(\mu - \mu_B B) + \frac{1}{2}\Phi_0(\mu + \mu_B B) \approx \Phi_0(\mu) - \frac{1}{2}(\mu B)^2 \frac{\partial N}{\partial \mu} \tag{1.84}$$

where we have made use of the second expression (1.83). At $T = 0$, $\mu = E_F$, meaning that we can write

$$\frac{\partial N}{\partial \mu} = \frac{\partial N}{\partial E_F} = g(E_F) = \frac{3N}{2E_F} \tag{1.85}$$

The magnetisation is given by

$$M = \frac{1}{V}\left(\frac{\partial \Phi}{\partial B}\right)_{T,V} = \mu_0 \mu_B^2 \frac{B}{V} \frac{\partial N}{\partial E_F} \tag{1.86}$$

such that the *magnetic susceptibility* for Pauli paramagnetism is given by

$$\boxed{\chi_{\text{Pauli}} = \mu_0 \frac{dM}{dB} = \frac{3}{2}\frac{n}{E_F}\mu_0 \mu_B^2} \tag{1.87}$$

We can also make a more qualitative argument using the fact that

$$M = -\frac{1}{V}\frac{dE}{dB} \backsim -(\#\text{ of up spins} - \#\text{ of down spins})\frac{\mu_B}{V} \tag{1.88}$$

and using similar reasoning as (1.76) with $\Delta E \backsim \mu_B B$. This obtains the same result as the above analysis. We shall study magnetic effects more closely in chapter 4.

2. *Periodic Structures*

This chapter introduces some of the ideas associated with periodic structures, including:

- Crystal Lattices
- Reciprocal Space
- Crystal Diffraction

None of the models introduced in the previous chapter feature any consideration of the periodic microscopic structure of materials, and hence all feature regimes in which their predictions depart from what is observed experimentally. Periodic structures underpin much of Condensed Matter physics, as most condensed phases consist of a set of regular, repeating 'blocks', and so we must build this into whatever theory we are using to describe our materials. Note that this chapter is very heavy on terminology, so it is recommended that readers familiarise themselves quickly with any italicised terms.

2.1 Crystal Lattices

A *crystal* is a homogeneous solid substance whose constituents are arranged in a highly ordered microscopic structure. In this context, the term crystal is not isolated to precious stones, but can in fact be used more generally to refer to any regularly ordered structure. We can describe such a structure as a *lattice*; a grid of points defined by a set of linearly independent *primitive lattice vectors* $\mathbf{a}_1$, $\mathbf{a}_2$ and $\mathbf{a}_3$. Then, a given position $\mathbf{R}$ within the lattice can be described as some linear combination of these lattice vectors

$$\boxed{\mathbf{R} = n_1\mathbf{a}_1 + n_2\mathbf{a}_2 + n_3\mathbf{a}_3} \tag{2.1}$$

where n_1, n_2 and n_3 are integers. Note that this choice of primitive lattice vectors is not unique in two- and three-dimensions. It also does not matter where we set $\mathbf{R} = 0$ within our system, so long as it coincides with one of the points on the lattice. This is a reflection of the fact that the lattice is homogeneous, and thus must appear the same regardless of the choice of origin. Implicit in this assumption is that the lattices that we are working with are semi-infinite, which shall remain an assumption throughout the remainder of this text.

2.1.1 Unit Cells

A *unit cell* of a lattice is any region of space that you can repeat over and over again to re-construct the entire lattice. As with the primitive lattice vectors, the choice of unit cell is not unique. A *primitive unit cell* contains only one total lattice point; it may contain fractions of lattice points that add up to a single total lattice point. A *conventional unit cell* usually contains more than one lattice point, but is easier to work with when it comes to constructing an appropriate set of lattice vectors.

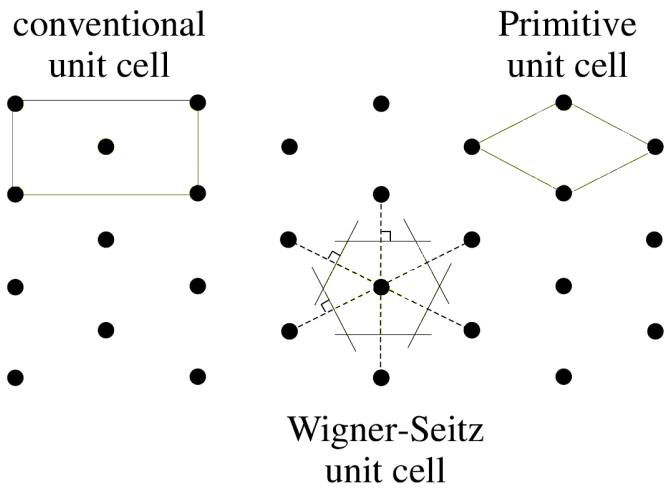

Figure 2.1: Examples of unit cells on some general lattice

There is a special type of cell called the *Wigner-Seitz* unit cell. This is the space that is closer to one lattice point that any other lattice point, such that it can be tiled to reconstruct the entire lattice. To construct this unit cell, one picks a lattice point, and draws perpendicular bisectors between it and neighbouring points. These lines form the boundaries of the Wigner-Seitz cell.

2.1.2 Lattices in Three-Dimensions

The lattice thus forms a grid of reference points. A *basis* is the description of objects in the unit cell relative to some point within the lattice. In this way, the entire crystal can be described by a combination of a lattice and a basis.

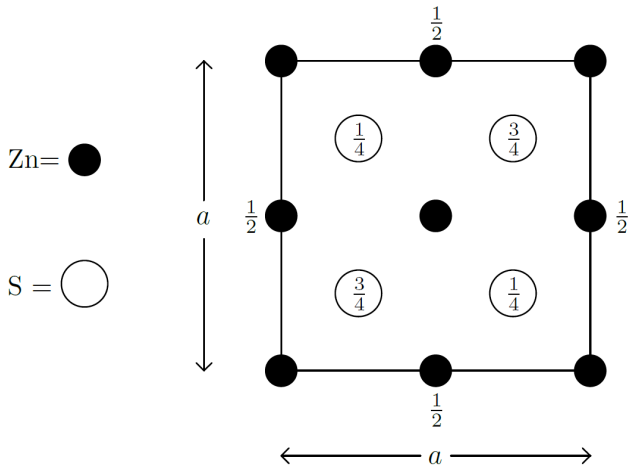

Figure 2.2: A cut of the zincblende (ZnS) lattice at $z = 0$. We take $\mathbf{e}_y$ vertically upwards along the page, and $\mathbf{e}_x$ horizontally along the page

Let us consider the example of zincblende, shown in figure 2.2. In this case, the unit cell will contain one atom of each type, and will be of length $a/2$. We thus adopt the primitive lattice vectors

$$\mathbf{a}_1 = \frac{a}{2}[1,1,0], \quad \mathbf{a}_2 = \frac{a}{2}[1,0,1], \quad \mathbf{a}_3 = \frac{a}{2}[0,1,1] \tag{2.2}$$

The distance a is known as the *lattice constant*. Without loss of generality, let us choose the origin of our coordinates at the bottom left-hand corner zinc atom. This means that the basis for this structure is

$$\text{zinc}: \quad a[0,0,0] \tag{2.3}$$

$$\text{sulfur}: \quad a\,[1/4,1/4,3/4] \tag{2.4}$$

Note that it is conventional to denote coordinates in the lattice using square brackets. Given this basis, we can write any point within the entire lattice

$$\mathbf{R}_{\text{zinc}} = a[n_1,n_2,n_3] \tag{2.5}$$

$$\mathbf{R}_{\text{sulfur}} = a[n_1,n_2,n_3] + a[1/4,1/4,3/4] \tag{2.6}$$

The *coordination number* of a lattice z is the number of nearest neighbours of any point within the lattice. For both zinc and sulfur within the above lattice, the coordination number is $z = 4$.

We have some more definitions. A *orthorhombic lattice* has orthogonal vectors all of different lengths. *Tetragonal lattices* have orthogonal vectors, two of which are the same length. A *simple cubic lattice* -you guessed it- has orthogonal lattice vectors that are all the same length. Simple cubic lattices are very rare, only occurring in polonium Po. This is because it requires a lot of space, as the packing is not very efficient, meaning that it is not an energetically favourable configuration for the system to reside in.

Body Centred Cubic Lattice

The body centred cubic (BCC) lattice is a simple cubic lattice where an additional point has been added in the very center of the cube (see figure 2.3). This is sometimes known as cubic-I. The conventional unit cell for this lattice contains exactly two lattice points. We have the primitive lattice vectors

$$\mathbf{a}_1 = a[1,0,0], \quad \mathbf{a}_2 = a[0,1,0], \quad \mathbf{a}_3 = a[1/2,1/2,1/2] \tag{2.7}$$

It is easy to check that any point in the lattice can be written in the form (2.1). Similarly, we have the basis:

$$\text{corner}: \quad a[0,0,0] \tag{2.8}$$
$$\text{center}: \quad a\,[1/2,1/2,1/2] \tag{2.9}$$

The coordination number of a BCC lattice is $z = 2^3 \times 1 = 8$, as there are two different signs that each of the coordinates may take ($\times 2^3$), but only one unique way of arranging the coordinates ($\times 1$).

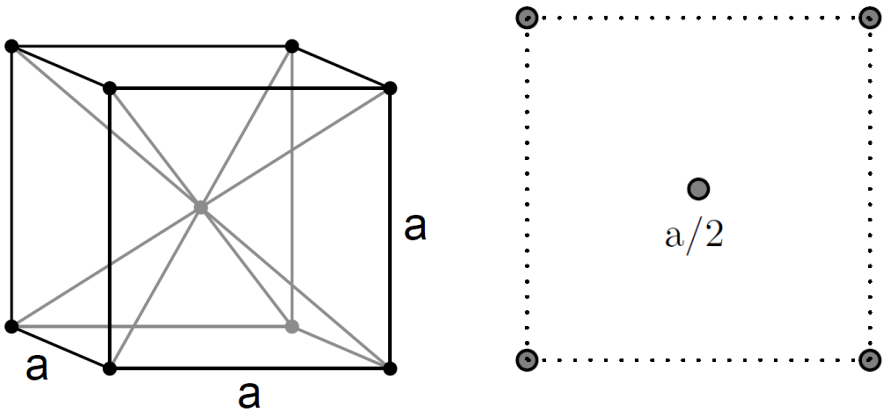

(a) (b)

Figure 2.3: The body centred cubic lattice (a) The unit cell (b) A plan view of the unit cell. Unlabelled points are both at heights 0 and a

Face Centred Cubic Lattice

The face centred cubic (FFC) lattice is a simple cubic lattice where there is an additional point in the center of every face of the cube (see figure 2.4). This is sometimes known as cubic-F, for 'face-centred'. The conventional unit cell for this lattice contains exactly four lattice points. We have the primitive lattice vectors

$$\mathbf{a}_1 = a[1/2,1/2,0], \quad \mathbf{a}_2 = a[1/2,0,1/2], \quad \mathbf{a}_3 = a[0,1/2,1/2] \tag{2.10}$$

Once again, it is easy to check that any point in the lattice can be written in the form (2.1). We have the basis

$$\text{corner}: \quad a[0,0,0] \tag{2.11}$$
$$\text{face-}xy: \quad a[1/2,1/2,0] \tag{2.12}$$
$$\text{face-}xz: \quad a[1/2,0,1/2] \tag{2.13}$$
$$\text{face-}yz: \quad a[0,1/2,1/2] \tag{2.14}$$

The coordination number of the FCC lattice is $z = 2^2 \times 3 = 12$, as there are two different signs each of the coordinates may take ($\times 2^2$), but three unique ways of arranging the coordinates ($\times 3$).

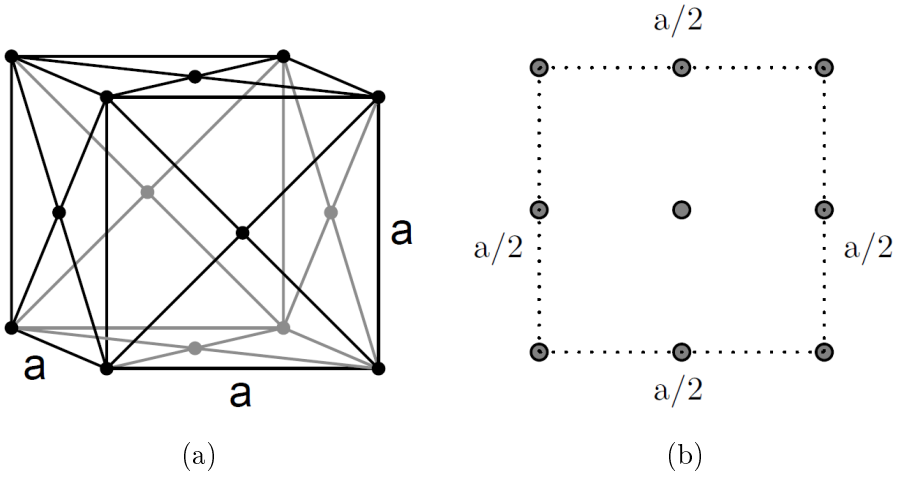

Figure 2.4: The face centred cubic lattice (a) The unit cell (b) A plan view of the unit cell. Unlabelled points are both at heights 0 and a

2.2 Reciprocal Space

The term *momentum* can be used quite generally to a conserved quantity that results from some symmetry in the system. For example, the familiar conservation linear momentum is a consequence of continuous translation symmetry in systems, while angular momentum is conserved due to a rotational symmetry of the system. How does this apply to periodic systems?

2.2.1 Crystal Momentum

Consider some Hamiltonian H on a crystal lattice. Let the translational evolution operator be

$$\mathrm{U}(\mathbf{a}) = e^{i\mathbf{a}\cdot\mathbf{p}/\hbar} \tag{2.15}$$

where $\mathbf{a}$ is some translation vector, and $\mathbf{p}$ is the momentum operator. Then, it is true that $[H, \mathrm{U}(\mathbf{a})] \neq 0$ for some general $\mathbf{a}$, meaning that $\mathbf{p}$ is not conserved in the lattice. However, we know that $[H, \mathrm{U}(\mathbf{R})] = 0$ (where $\mathbf{R}$ is as defined in (2.1)) as the system must be invariant under translation by some lattice vector $\mathbf{R}$. Suppose that we have some operator $\Lambda_{\mathbf{R}}$ that generates lattices translations, satisfying

$$\Lambda_{\mathbf{R}}\psi(\mathbf{r}) = \psi(\mathbf{r}+\mathbf{R}), \quad \psi(\mathbf{r}) = \langle \mathbf{r}|\psi\rangle \tag{2.16}$$

where $|\psi\rangle$ is some state of the system. Consider some other state $|\phi\rangle$. Then:

$$\langle\phi_{\mathbf{r}}|\,\Lambda_{-\mathbf{R}}\,|\psi_{\mathbf{r}'}\rangle = \langle\phi_{\mathbf{r}}|\psi_{\mathbf{r}'-\mathbf{R}}\rangle = \langle\phi_{\mathbf{r}+\mathbf{R}}|\psi_{\mathbf{r}'}\rangle = \langle\phi_{\mathbf{r}}|\,\Lambda^{\dagger}_{\mathbf{R}}\,|\psi_{\mathbf{r}'}\rangle \tag{2.17}$$

where the third expression follows from making a lattice-invariant shift in coordinates. This allows us to conclude that

$$\Lambda_{\mathbf{R}}\Lambda^{\dagger}_{\mathbf{R}} = \mathbf{I} \tag{2.18}$$

meaning that the lattice translation operator is unitary. As $\Lambda_{\mathbf{R}} = \mathrm{U}(\mathbf{R})$, we have that $[H, \Lambda_{\mathbf{R}}] = 0$. This means that $\psi(\mathbf{r})$ must be an eigenstate of $\Lambda_{\mathbf{R}}$ if it is an eigenstate of H:

$$\Lambda_{\mathbf{R}}\psi(\mathbf{r}) = \lambda_{\mathbf{R}}\psi(\mathbf{r}) \tag{2.19}$$

If follows that

$$\Lambda^{\dagger}_{\mathbf{R}}\Lambda_{\mathbf{R}}\psi(\mathbf{r}) = \psi(\mathbf{r}) = \lambda^{*}_{\mathbf{R}}\lambda_{\mathbf{R}}\psi(\mathbf{r}) \quad \longrightarrow \quad \lambda_{\mathbf{R}} = e^{i\phi} \tag{2.20}$$

for some phase ϕ. Since this translation is discrete, making two successive translations by $\mathbf{R}$ is equivalent to making a single translation by $2\mathbf{R}$:

$$\Lambda^{2}_{\mathbf{R}} = \Lambda_{2\mathbf{R}} \tag{2.21}$$

This restricts ϕ to being a linear function of $\mathbf{R}$, and a scalar. However, we also want our lattice to be completely invariant under translations in $\mathbf{R}$. Comparing (2.16) and (2.19), we thus define some $\mathbf{G}$ that satisfies

$$\boxed{e^{i\mathbf{G}\cdot\mathbf{R}} = 1} \tag{2.22}$$

The *reciprocal lattice* is the set of points denoted by $\mathbf{G}$ that satisfies the above equation for all points $\mathbf{R}$ on the *direct lattice* (we have thus far been referring to this simply as the lattice). The *reciprocal lattice vector* $\mathbf{G}$ is usually written as

$$\boxed{\mathbf{G} = h\mathbf{b}_1 + k\mathbf{b}_2 + \ell\mathbf{b}_3} \tag{2.23}$$

for constant coefficients h, k and ℓ. In order for the definition of the reciprocal lattice (2.22) to be satisfied, we require that

$$2\pi m = \mathbf{G}\cdot\mathbf{R} = (hn_1\,\mathbf{a}_1\cdot\mathbf{b}_1 + kn_2\,\mathbf{a}_2\cdot\mathbf{b}_2 + \ell n_3\,\mathbf{a}_3\cdot\mathbf{b}_3 + \text{mixed terms}) \tag{2.24}$$

for some integer m. We argue that the vectors $\mathbf{a}_i$ and $\mathbf{b}_j$ must satisfy the orthogonality relationship

$$\mathbf{a}_i\cdot\mathbf{b}_j = 2\pi\delta_{ij} \tag{2.25}$$

which corresponds to the condition that the points are either on the reciprocal lattice, or not. With this definition, all mixed terms in $\mathbf{a}_i$ and $\mathbf{b}_j$ disappear, and we obtain

$$2\pi m = 2\pi(hn_1 + kn_2 + \ell n_3) \tag{2.26}$$

This allows us to conclude that coefficients h, k, and ℓ are integers, known as the *Miller indices*. Furthermore, the condition (2.25) implies that $\mathbf{b}_j$ are the reciprocal vectors, given by

$$\mathbf{b}_1 = 2\pi\frac{\mathbf{a}_2\times\mathbf{a}_3}{\mathbf{a}_1\cdot(\mathbf{a}_2\times\mathbf{a}_3)},\quad \mathbf{b}_2 = 2\pi\frac{\mathbf{a}_3\times\mathbf{a}_1}{\mathbf{a}_1\cdot(\mathbf{a}_2\times\mathbf{a}_3)},\quad \mathbf{b}_3 = 2\pi\frac{\mathbf{a}_1\times\mathbf{a}_2}{\mathbf{a}_1\cdot(\mathbf{a}_2\times\mathbf{a}_3)} \tag{2.27}$$

These are the formulae for three dimensions. In two dimensions, one simply replaces $\mathbf{e}_3$ by $\mathbf{e}_z$ to restrict consideration to the x-y plane.

We have thus shown that in a lattice, normal momentum is not conserved. However, we have shown that there is some quantity that is conserved due to the symmetry of the lattice under the lattice translation operator $\Lambda_{\mathbf{R}}$. This is the wavevector $\mathbf{k}$ that is conserved modulus $\mathbf{G}$, known as the *crystal momentum*.

2.2.2 As a Fourier Transform

Consider some function on the reciprocal lattice $\rho(\mathbf{r})$ (such as the density of atoms) which by definition must be periodic in the lattice vector $\mathbf{R}$, such that $\rho(\mathbf{r}) = \rho(\mathbf{r}+\mathbf{R})$. Its Fourier transform is given by

$$\widetilde{\rho}(\mathbf{k}) = \int d^3\mathbf{r}\, e^{i\mathbf{k}\cdot\mathbf{r}}\rho(\mathbf{r}) \tag{2.28}$$

The integral sum over all space can be broken up into a sum of integrals over each unit cell. We write any point $\mathbf{r}$ as the sum of some lattice point $\mathbf{R}$ and a vector $\mathbf{x}$ within the unit cell

$$\widetilde{\rho}(\mathbf{k}) = \sum_{\mathbf{R}}\int_{\text{unit cell}} d^3\mathbf{x}\, e^{i\mathbf{k}(\mathbf{x}+\mathbf{R})}\rho(\mathbf{x}+\mathbf{R}) = \sum_{\mathbf{R}} e^{i\mathbf{k}\cdot\mathbf{R}}\int_{\text{unit cell}} d^3\mathbf{x}\, e^{i\mathbf{k}\cdot\mathbf{x}}\rho(\mathbf{x}) \tag{2.29}$$

where we have used the fact that ρ is invariant under lattice translations. The first sum is over a series of oscillating functions, which only produce a non-zero value if $\mathbf{k}$ is on the reciprocal lattice. This means that it is simply a sum over delta functions. We thus re-write this expression as

$$\widetilde{\rho}(\mathbf{k}) = (2\pi)^3\sum_{\mathbf{G}}\delta^3(\mathbf{k}-\mathbf{G})\left(\int_{\text{unit cell}} d^3\mathbf{x}\, e^{i\mathbf{k}\cdot\mathbf{x}}\rho(\mathbf{x})\right) \tag{2.30}$$

The bracketed term is known as the *structure factor*, which tells us about how the unit cell is represented in reciprocal space. This will become important in section 2.3. From this expression, it is also possible to show that the reciprocal lattice has all the symmetries of the direct lattice, as well as inversion symmetry ($\mathbf{k}\mapsto-\mathbf{k}$). This means, for example, that a system that is periodic in a in real space is periodic in $2\pi/a$ in reciprocal space.

2.2.3 The Brillouin Zone

The *Brillouin zone* is the unit cell of the reciprocal lattice. The conservation of crystal momentum means that waves in the direct lattice are unchanged if their wavevector is shifted in the reciprocal lattice by $\mathbf{k} \mapsto \mathbf{k} + \mathbf{G}$. The Brillouin zone thus contains each physically different crystal momentum exactly once; each $\mathbf{k}$ point within the Brillouin zone is physically different, and all physically different points occur once within the zone.

The *first Brillouin zone* in reciprocal space is the Wigner-Seitz cell in the reciprocal lattice, constructed in the completely analogous way. Higher (second, third, ...) Brillouin zones are constructed by performing the Wigner-Seitz process on the next nearest neighbours. An example of this is shown in figure 2.5 below. Opposing Brillouin zones boundaries are connected by a reciprocal lattice vector, meaning that they are at points satisfying $|\mathbf{k}| = |\mathbf{k} + \mathbf{G}|$. We note that all Brillouin zones have the same area, meaning that they contain the same number of $\mathbf{k}$ states.

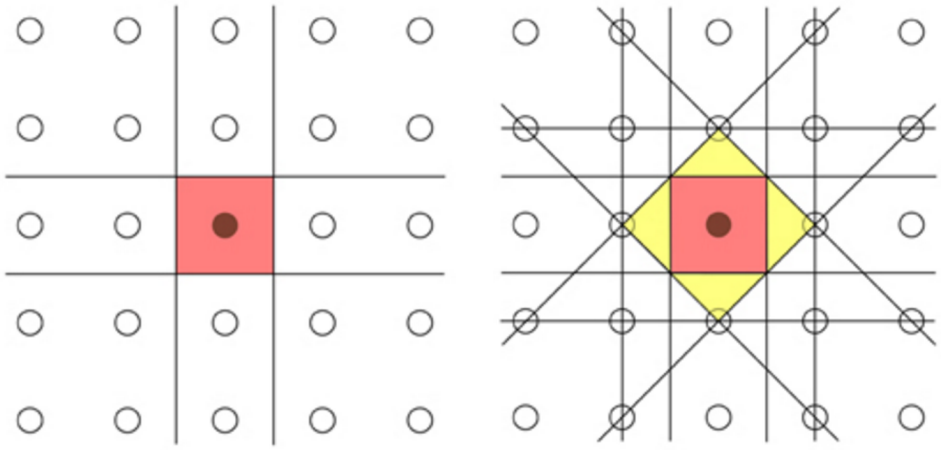

(a) (b)

Figure 2.5: The construction of the first and second Brillouin zones for a 2D square lattice. More examples can be found at https://www.doitpoms.ac.uk/tlplib/brillouin_zones/zone_construction.php

Now, exactly how many states are there in each Brillouin zone? By the definition of the reciprocal vectors, the first Brillouin zone has a $\mathbf{k}$-space volume of

$$V_{\mathbf{k}} = \mathbf{b}_1 \cdot (\mathbf{b}_2 \times \mathbf{b}_3) \tag{2.31}$$

Now, let us involve the periodic boundary conditions associated with the lattice (sometimes known as *Born von Karman* boundary conditions). Consider a plane wave

$$\psi(\mathbf{r}) = e^{i(\mathbf{k}\cdot\mathbf{r} - \omega t)}, \quad \phi(\mathbf{r} + N_j \mathbf{a}_j) = \phi(\mathbf{r}) \tag{2.32}$$

where N_j is the number of primitive unit cells in the j-th direction, and $\mathbf{a}_j$ is the lattice vector in the j-th direction. Then, the total number of primitive unit cells in the sample N is clearly given by $N = N_1 N_2 N_3$. Substituting the plane wave (2.32) into the periodic boundary condition, we have that

$$e^{iN_j \mathbf{k}\cdot\mathbf{a}_j} = 1 \tag{2.33}$$

The condition of the reciprocal lattice (2.22) must still be satisfied, meaning that the allowed wavevectors are given by

$$\mathbf{k} = \sum_j \frac{m_j}{N_j}\mathbf{b}_j \tag{2.34}$$

where m_j corresponds to the j-th Miller index. Each time that m_j is change by one, we generate a new $\mathbf{k}$ state. This means that the $\mathbf{k}$ space volume occupied by a single state is

$$V_{\mathbf{k}1} = \frac{\mathbf{b}_1}{N_1} \cdot \left(\frac{\mathbf{b}_2}{N_2} \times \frac{\mathbf{b}_3}{N_3}\right) = \frac{V_\mathbf{k}}{N} \quad \longrightarrow \quad \frac{V_\mathbf{k}}{V_{\mathbf{k}1}} = N \tag{2.35}$$

This means that the Brillouin zone contains the same number of $\mathbf{k}$ states are the number of primitive unit cells that make up the lattice.

Lastly, an important - but useful - fact to remember is that the reciprocal lattice for the cubic is the cubic lattice itself, and that the BCC and FCC lattices are each others' reciprocal lattice.

2.2.4 Lattice Planes

A *lattice plane* (sometimes referred to as a *crystal plane*) is any plane that contains three or more non-collinear points on the direct lattice. These have a normal given by the reciprocal lattice vector $\mathbf{G}$, meaning that the set of Miller indices $(hk\ell)$ specify a particular family of lattice planes by defining their corresponding normal, and that each point on the reciprocal lattice corresponds to a lattice plane in the direct lattice. We can show this explicitly. For a given plane in the family $(hk\ell)$, the primitive lattice vectors $\mathbf{a}_1$, $\mathbf{a}_2$ and $\mathbf{a}_3$ will intercept the axes in the ratio

$$\frac{|\mathbf{a}_1|}{h} : \frac{|\mathbf{a}_2|}{k} : \frac{|\mathbf{a}_3|}{\ell} \tag{2.36}$$

Then, define the vectors in the plane

$$\mathbf{r}_1 = \frac{\mathbf{a}_1}{h} - \frac{\mathbf{a}_2}{k}, \quad \mathbf{r}_2 = \frac{\mathbf{a}_1}{h} - \frac{\mathbf{a}_3}{\ell} \tag{2.37}$$

that do not lie parallel to one another, by definition of the primitive lattice vectors. Then, by the definition of the reciprocal lattice vector (2.23), it is clear that

$$\mathbf{G} \cdot \mathbf{r}_1 = \mathbf{G} \cdot \mathbf{r}_2 = 0 \tag{2.38}$$

Thus, as we have shown that $\mathbf{G}$ is perpendicular to two non-parallel vectors in the plane, it must be perpendicular to the plane. One can also show that the $\mathbf{R} = [hk\ell] = h\mathbf{a}_1 + k\mathbf{a}_2 + \ell\mathbf{a}_3$ direction is parallel to the $\mathbf{G} = (hk\ell) = h\mathbf{b}_1 + k\mathbf{b}_2 + \ell\mathbf{b}_3$ direction by showing that $\mathbf{R} \cdot \mathbf{G} = |\mathbf{R}||\mathbf{G}|$.

Conventionally, the $(hk\ell)$ are always expressed as being divided through by their lowest common multiple so as to avoid the over-counting of lattice planes. Furthermore, the Miller indices of BCC and FCC lattices are often stated as in (2.23) using the primitive lattice vectors of the cubic lattice, meaning that not all possible combinations of Miller indices are actually lattice planes for both the BCC and FCC lattice. When drawing lattice planes, a useful trick to remember is that the Miller indices denote the number of planes encountered when moving a unit along that direction. For example, (120) means that one will encounter one lattice plane when moving a unit along $\mathbf{e}_1$, but two when moving a unit along $\mathbf{e}_2$.

Distances between Lattice Planes

Let us consider the separation between neighbouring lattice planes within a given family. Again, for a family of lattice planes $(hk\ell)$, at least one of the Miller indices is non-zero, and so without loss of generality assume that $h \neq 0$. The corresponding family of planes divides the vector $\mathbf{a}_1$ into h parts of equal length, meaning that $\mathbf{R}_1 = 0$ ends on one plane, and $\mathbf{R}_2 = \mathbf{a}_1/h$ ends on another. Thus, the projection of

$$\mathbf{R}_2 - \mathbf{R}_1 = \frac{\mathbf{a}_1}{h} \tag{2.39}$$

onto $\mathbf{G}$ (which is the perpendicular to all the planes) will give the distance between the neighbouring planes. Thus

$$d_{hk\ell} = \left| \frac{\mathbf{a}_1}{h} \cdot \frac{\mathbf{G}}{|\mathbf{G}|} \right| = \left| \frac{\mathbf{a}_1}{h} \cdot \frac{(h\mathbf{b}_1 + k\mathbf{b}_2 + \ell\mathbf{b}_3)}{|\mathbf{G}|} \right| \tag{2.40}$$

Using the orthogonality relationship (2.25), we find that

$$\boxed{d_{hk\ell} = \frac{2\pi}{|\mathbf{G}|} = \frac{2\pi}{\sqrt{h^2|\mathbf{b}_1|^2 + k^2|\mathbf{b}_2|^2 + \ell^2|\mathbf{b}_3|^2}}} \tag{2.41}$$

This is the general result that is satisfied for any crystal structure. For an orthorhombic lattice, $|\mathbf{b}_i| = 2\pi/|\mathbf{a}_i|$, as the axes are orthogonal. This means that

$$\frac{1}{d_{hk\ell}^2} = \frac{h^2}{|\mathbf{a}_1|^2} + \frac{k^2}{|\mathbf{a}_2|^2} + \frac{\ell^2}{|\mathbf{a}_3|^2} \tag{2.42}$$

is the relationship for orthorhombic crystals. For cubic crystals, $|\mathbf{a}_1| = |\mathbf{a}_2| = |\mathbf{a}_3| = a$ for some lattice constant a, such that

$$d_{hk\ell} = \frac{a}{\sqrt{h^2 + k^2 + \ell^2}} \tag{2.43}$$

for cubic crystals. This is usually the case that we will be considering throughout the remainder of this text.

2.3 Crystal Diffraction

The last two sections were focussed on building an understanding of the internal structures of crystals, and how the direct lattice is intimately linked to what we call the reciprocal lattice. Using this knowledge, we shall now examine how we experimentally investigate the internal structure of crystals using diffraction.

2.3.1 The Laue Condition

Suppose that we expose a crystal to radiation (not necessarily light), with incoming wavevector $\mathbf{k}$. Let $\mathbf{k}'$ be the wavevector of the outgoing, scattered radiation. We shall be considering the case of elastic scattering, meaning that $|\mathbf{k}| = |\mathbf{k}'|$. Fermi's Golden rule gives us the transition rate into a particular scattered state as

$$\Gamma(\mathbf{k}, \mathbf{k}') = \frac{2\pi}{\hbar} \left|\langle \mathbf{k}' | \, V \, | \mathbf{k} \rangle\right|^2 \delta(E_{\mathbf{k}'} - E_{\mathbf{k}}) \tag{2.44}$$

where $V = V(\mathbf{r})$ is the scattering potential in which we encode the information about the crystal structure. In $\mathbf{k}$-space representation, this matrix element is given by Fourier transform

$$\langle \mathbf{k}' | \, V \, | \mathbf{k} \rangle = \frac{1}{L^3} \int d^3\mathbf{r} \, e^{-i(\mathbf{k}-\mathbf{k}')\cdot\mathbf{r}} \, V(\mathbf{r}) \tag{2.45}$$

where L is the one-dimensional system size. As usual, we can decompose this integral into a sum over lattice vectors and unit cells using the fact that $V(\mathbf{r}) = V(\mathbf{r} + \mathbf{R})$ as it represents the potential of the lattice.

$$\langle \mathbf{k}' | \, V \, | \mathbf{k} \rangle = \frac{1}{L^3} \sum_{\mathbf{R}} e^{-i(\mathbf{k}-\mathbf{k}')\cdot\mathbf{R}} \int\limits_{\text{unit cell}} d^3\mathbf{x} \, e^{-i(\mathbf{k}-\mathbf{k}')\cdot\mathbf{x}} V(\mathbf{x}) \tag{2.46}$$

Once again, the sum over $\mathbf{R}$ will evaluate to zero, unless the relationship

$$\boxed{\Delta\mathbf{k} = \mathbf{k} - \mathbf{k}' = \mathbf{G}} \tag{2.47}$$

is satisfied, allowing the terms in the sum to interfere constructively. This is known as the *Laue condition* for diffraction. This condition is precisely a statement of the conservation of crystal momentum.

Equivalence of Bragg and Laue Conditions

Consider figure 2.6 below. $\mathbf{G}$ corresponds to a particular family of lattice planes, with separation d given by (2.41).

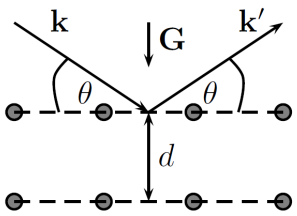

Figure 2.6: Diffraction from a crystal lattice

Let $\mathbf{e_k}$, $\mathbf{e_{k'}}$ and $\mathbf{e_G}$ be the unit vectors for $\mathbf{k}$, $\mathbf{k}'$ and $\mathbf{G}$ respectively. From geometry, we have that

$$\mathbf{e_k} \cdot \mathbf{e_G} = -\mathbf{e_{k'}} \cdot \mathbf{e_G} = \sin\theta \tag{2.48}$$

Suppose that the Laue condition (2.47) is satisfied, and that the incoming radiation satisfies $|\mathbf{k}| = |\mathbf{k}'| = 2\pi/\lambda$ for some wavelength λ. Then, the Laue condition can be re-written as

$$\frac{2\pi}{\lambda}(\mathbf{e_k} - \mathbf{e_{k'}}) = \mathbf{G} \quad \longrightarrow \quad \mathbf{e_G} \cdot \frac{2\pi}{\lambda}(\mathbf{e_k} - \mathbf{e_{k'}}) = \frac{2\pi}{\lambda}(2\sin\theta) = \mathbf{e_G} \cdot \mathbf{G} = |\mathbf{G}| \tag{2.49}$$

This means that

$$\frac{2\pi}{|\mathbf{G}|}(2\sin\theta) = 2d\sin\theta = \lambda \tag{2.50}$$

which is the familiar Bragg diffraction condition for constructive interference. This means that the Laue and Bragg conditions are equivalent; one can say that diffraction either occurs when the interference is constructive, or when crystal momentum is conserved.

Using the Laue Condition

One can use the Laue condition to find the allowed diffraction planes for a given wavelength and crystal sample, by using the *Ewald construction*:

1. Draw, and label, the reciprocal lattice points
2. Draw an incoming wavevector $\mathbf{k}$ that ends at the origin
3. Carefully construct a circle/sphere (the *Ewald sphere*) of radius $2\pi/\lambda$ around the starting point of $\mathbf{k}$
4. Rotate the crystal around (000) until it intersects with a reciprocal lattice point; the corresponding lattice plane is allowed in diffraction

This technique is quite fiddly, and requires very careful sketching; a ruler is definitely recommended. Note that in such a sketch, $\mathbf{k}$, $\mathbf{k}'$ and $\mathbf{G}$ should form an isosceles triangle with angle 2θ between $\mathbf{k}$ and $\mathbf{k}'$ at the origin.

2.3.2 Diffraction Intensity

Imposing the Laue condition, we can write (2.46) as

$$\langle \mathbf{k}' | \, V \, | \mathbf{k} \rangle = \frac{1}{L^3} \sum_{\mathbf{R}} e^{-i\mathbf{G}\cdot\mathbf{R}} \int_{\text{unit cell}} d^3\mathbf{x} \, e^{-i\mathbf{G}\cdot\mathbf{x}} \, V(\mathbf{x}) \tag{2.51}$$

This means that the structure factor for the diffraction is given by

$$\boxed{S_{hk\ell}(\mathbf{G}) = \int_{\text{unit cell}} d^3\mathbf{x} \, e^{-i\mathbf{G}\cdot\mathbf{x}} \, V(\mathbf{x})} \tag{2.52}$$

As Fermi's golden rule gives us the rate of scattering, we write the scattering intensity as $I_{hk\ell} \propto |S_{hk\ell}|^2$; that is, the intensity resulting from a diffraction off a the crystal planes $(hk\ell)$ is proportional to the square of the associated structure factor.

X-ray Scattering

X-rays scatter from the electrons within the lattice, meaning that one can take the scattering potential $V(\mathbf{x})$ as being proportional to the electron density:

$$V(\mathbf{x}) \backsim \sum_j Z_j \, g_j(\mathbf{x} - \mathbf{x}_j) \tag{2.53}$$

where Z_j is the atomic number of atom j *within the unit cell*, and g_j is some short-ranged function. The corresponding structure factor is then given by

$$S(\mathbf{G}) \backsim \sum_j f_j(\mathbf{G})\, e^{i\mathbf{G}\cdot\mathbf{x}_j} \tag{2.54}$$

f_j is known as the *form factor*, and is roughly proportional to Z_j, but with some dependence on the magnitude of $\mathbf{G}$. Suppose that a given atom j is located at $\mathbf{x}_j = [x_j, y_j, z_j]$. Then, our form-factor becomes

$$S_{hkl} = \sum_j f_j\, e^{2\pi i(hx_j + ky_j + \ell z_j)} \tag{2.55}$$

We shall now consider some cases of this expression:

- Cubic lattice - This has a basis $[0,0,0]$, as there are only atoms at the corners of the unit cell. This means that the structure factor can be written as

$$S^{(\mathrm{C})}_{hk\ell} = \sum_j f_j \tag{2.56}$$

- BCC lattice - We shall consider a BCC lattice where all atoms are of the same type, and thus have the same structure factor f_j. Adopting the usual basis $[0,0,0]$, $[1/2,1/2,1/2]$, the structure factor becomes

$$S^{(\mathrm{BCC})}_{hk\ell} = f_j\left[1 + (-1)^{(h+k+\ell)}\right] \tag{2.57}$$

  This means that for odd $(h+k+\ell)$, there is no diffraction intensity. This is known as a *systematic absence*

- FCC lattice - We shall again consider an FCC lattice where all atoms are of the same type, with the same structure factor f_j. Adopting the usual basis $[0,0,0]$, $[1/2,1/2,0]$, $[1/2,0,1/2]$, $[0,1/2,1/2]$, the structure factor becomes

$$S^{(\mathrm{FCC})}_{hk\ell} = f_j\left[1 + (-1)^{(h+k)} + (-1)^{(h+\ell)} + (-1)^{(k+\ell)}\right] \tag{2.58}$$

  This means that for mixed odd/even h, k, and ℓ, we have another systematic absence

We thus have the following selection rules for X-ray diffraction:

Lattice Structure	Allowed Reflections
Cubic	All reflections are possible
BCC	Only reflections when $h+k+\ell = 2n$ for integer n
FCC	Only reflections when $hk\ell$ are all odd or all even

Table 2.1: Diffraction selection rules

However, from the derivations given above, it appears that these selection rules only apply when the atoms within the BCC and FCC lattices are the same. However, these are in fact very general results, as we shall now demonstrate. Recall the definition of the structure factor (2.52). We argue that the potential $V(\mathbf{x})$ can be written as a convolution of the lattice structure, and the atoms that make up the basis, according to

$$V(\mathbf{x}) = \int d^3\mathbf{x}'\, V_{\text{lattice}}(\mathbf{x}')V_{\text{basis}}(\mathbf{x}-\mathbf{x}') \tag{2.59}$$

Now, the structure factor is clearly a Fourier transform of the potential, which means that by the convolution theorem

$$S_{hk\ell} = \left(S_{hk\ell}^{(\text{lattice})}\right)\left(S_{hk\ell}^{(\text{basis})}\right) \tag{2.60}$$

We can then argue that both V_{lattice} and V_{basis} are delta-function localised, but that V_{lattice} mus be independent of form factors, such that they only occur within the second bracket above. This means that the selection rules will hold in general, such that any systematic absence due to the lattice will be observed independent of the basis adopted.

X-rays for such diffraction experiments are generally produced in X-ray tubes. However, the beam is often divergent, and can contain multiple wavelengths, as well as Bremsstrahlung radiation (see B3 notes for more details). These hamper our ability to use X-rays for analysis, as the beam divergence creates a range of incident angles, while the spectral contamination means that the sample diffracts multiple wavelengths of radiation. These problems are usually solved by the use of limiting optics.

Neutron Scattering

Since neutrons are uncharged, the scatter from the nucleus due to the action of nuclear forces. As a result, the scattering potential is essentially a delta function, meaning that

$$V(\mathbf{x}) = \sum_j b_j\, \delta^3(\mathbf{x} - \mathbf{x}_j) \tag{2.61}$$

where b_j is the *nuclear scattering length* for neutrons. This means that we obtain the structure factor

$$S(\mathbf{G}) \backsim \sum_j b_j\, e^{i\mathbf{G}\cdot\mathbf{x}_j} \tag{2.62}$$

As the form of this expression is identical to (2.54) apart from b_j, the selection rules in table 2.1 will also hold for neutron diffraction.

Neutrons for such diffraction experiements can either be product as a by-product in nuclear reactors, or by accelerating protons into a stationary target to emit neutrons (known as *spallation*). These can be made monochromatic by either diffraction through a known crystal, or selecting the neutrons based on speed (select only neutrons that arrive at a particular time, as these must have the same energies).

Comparison of X-ray and Neutron Scattering

- For X-rays, the form factor $f_j \backsim Z_j$, meaning that the X-rays scatter more strongly from heavier atoms, and hardly at all from light atoms. This means that it is very difficult to see atoms of lower Z, as well as to distinguish between atoms of similar Z, as they will scatter by the same amount. On the other hand, the nuclear scattering length b_j varies erratically with Z. In particular, hydrogen scatters well, and so can easily be seen by neutrons (but not X-rays), and neutrons are able to distinguish atoms of close Z quite easily

- For neutrons, the scattering is very short ranged as previously discussed, meaning that there is no dependence on $\mathbf{G}$. However, for X-rays, $f_j = f_j(\mathbf{G})$, which makes exact calculations of diffraction amplitudes more complicated

- Unlike X-rays, neutrons have spin, meaning that diffraction experiments with neutrons can inform us about the spin states of the material

- Inelastic neutron scattering is much better technique than X-ray scattering for the observation of phonons, as the X-rays have a very small cross-section for exciting phonons due to the large energy range involved ($E = \hbar|\mathbf{k}|c$), meaning that it is hard to measure the phonon dispersion relation that results from the scattering. It is also easier to build a detector that measures neutron energy than one for X-rays

2.3.3 X-ray Powder Diffraction

Powder diffraction (the *Debye-Scherrer method*) involves scattering from a powdered sample, meaning that waves can scatter off small crystallites which may be orientated in any particular direction. Placing a piece of X-ray photographic film behind the powdered sample, we observe a series of concentric rings, the intensity of which can be measured. Using this information, and knowledge of the wavelength of the source, it is possible to determine the lattice spacings. For this, let us consider table 2.2 below.

$(hk\ell)$	$N = h^2 + k^2 + \ell^2$	Multiplicity	Cubic	BCC	FCC
100	1	6	✓		
110	2	12	✓	✓	
111	3	8	✓		✓
200	4	6	✓	✓	✓
210	5	24	✓		
211	6	24	✓	✓	
220	8	12	✓	✓	✓
221	9	24	✓		
300	9	6	✓		
310	10	24	✓	✓	
311	11	24	✓		✓
222	12	8	✓	✓	✓
...	...	...	...	...	...

Table 2.2: Diffraction selection rules. The checkmarks correspond to allowed diffractions

Note that we have added a column called the *multiplicity*. This quantity is important for calculating scattering amplitudes in powder diffraction experiments (and *only* in powder diffraction experiments), of the number of orientations of a family of lattice planes that are possible. Multiplicity is calculated in a very similar way to the coordination number z, by taking into account the number of permutations of $(hk\ell)$. For example, (100) has a multiplicity of $(3!/2!) \times 2^1 = 6$ as there are $3!/2!$ ways of arranging the integers, and 2^1 combinations of positive and negative. Taking account of multiplicity, we should then write the intensity as $\boxed{I_{hk\ell} \propto M_{hk\ell} \, |S_{hk\ell}|^2}$, where $M_{hk\ell}$ is the multiplicity factor. Let us now consider an example to illustrate how to perform analysis of an X-ray powder diffraction experiment.

A collimated beam of monochromatic X-rays of wavelength 0.162 *nm is incident upon a powdered sample of the cubic metal palladium Pd. Peaks in the diffracted X-ray pattern are observed at angles of* 42.3°, 49.2°, 72.2°. 87.4° *and* 92.3° *from the direction of the incident beam. Identify the lattice type, and calculate the lattice constant. How does this compare with known data, given that the density of Pd is* 12023 kgm^{-3}*?*

This problem is most easily tackled using a table such as 2.3 below. The first and second column labels the diffraction peaks, and their corresponding diffraction angle from the data. The factor of two in the angle is because one usually measures 2θ experimentally.

Peak	2θ	d (Å)	$(d_a/d)^2$	$3(d_a/d)^2$	N	$(hk\ell)$	a (Å)
a	42.3°	2.25	1	3	3	(111)	3.90
b	49.2°	1.96	1.33	3.99	4	(200)	3.90
c	72.2°	1.37	2.67	8.01	8	(220)	3.87
d	87.4°	1.17	3.67	11.01	11	(331)	3.88
e	92.3°	1.12	3.99	11.97	12	(222)	3.88

Table 2.3: An example table used to analyse X-ray powder diffraction data

In the third column, we calculate the lattice spacing from the Bragg condition $d = \lambda/(2\sin\theta)$, while the fourth column is the ratio of the calculated lattice spacing d to the lattice spacing of the first peak. We then recognise that these numbers are roughly integers if we multiply them by three, to give the integers N. Looking at table 2.2 gives the Miller indices in the seventh column, and allows us to conclude that the lattice is an FCC, as it displays the allowed reflections corresponding to an FCC crystal. Lastly, we calculate the lattice constants a in the last column by inverting (2.43) $a = d\sqrt{h^2+k^2+\ell^2}$.

Taking the average of the last column, we find an experimental value for the lattice constant of

$$a = (3.89 \pm 0.02)\ \text{Å} \tag{2.63}$$

Now, we can calculate the number density of Pd ($A = 106.4$) from the data as

$$n = \frac{\rho}{m} = \frac{12023\ \text{kgm}^{-3}}{(106.4)(1.66\times10^{-27}\ \text{kg})} = 6.8\times10^{28}\ \text{m}^{-3} \tag{2.64}$$

Given that Pd is an FCC crystal, there are four atoms per unit cell, meaning that

$$a_c^{-3} = \frac{n}{4} \quad\longrightarrow\quad a_c = 3.89\ \text{Å} \tag{2.65}$$

This means that our value for the lattice constant obtained from experiment agrees with the calculated value within its margin of error.

On an experimental note, the diffraction rings from which the intensity can be deduced get fainter as the angle from the axis is increased. However, in order to make a more accurate prediction of the lattice constant, one needs to include more diffraction peaks/orders into the calculation. This means that to increase the accuracy of our experiment, the X-ray intensity could be increased to allow us to observe more diffraction peaks. For more information regarding experimental procedure, it is advised that readers consult the resources pertaining to ‘SS16: X-ray Diffraction‘ on the Oxford Practical Course website.

3. *Modelling Solids*

This chapter introduces some of the basic models associated with solids in Condensed Matter Physics, including:

- Atomic Chains
- Electrons in a Periodic Potential
- Band Theory and Semiconductors

We now have an understanding of crystal structures, and the relationship between the direct and reciprocal lattices in crystals. Armed with this knowledge, we shall examine some models of various properties of solids in attempt to improve on the models proposed in chapter 1. We shall see that including a consideration of the periodic nature of solid crystals makes for a much more accurate prediction of the material properties.

3.1 Atomic Chains

In this section, we consider a detailed model of vibration in a solid by examining one-dimensional atomic chains. In particular, we shall examine the behaviour of this system in terms of *normal modes* (collective oscillations of the system in which all parts move with the same frequency and fixed phase relation) and *phonons* (a discrete quantum of vibration that can be described by Bose-Einstien statistics). We met the latter of these when studying the Debye Model of heat capacity 1.2.3.

3.1.1 Monatomic Chain

Consider the case of a one-dimensional chain of N atoms of mass m, each connected by classical springs of spring constant κ, as in figure 3.1 below. Suppose that the atoms are separated by an equilibrium distance a. This can be thought of as our lattice constant, and the dotted box one possible unit cell for the system.

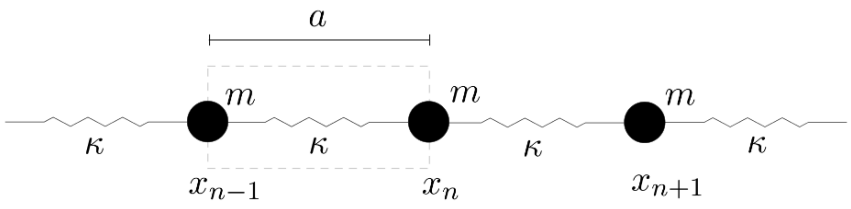

Figure 3.1: A schematic diagram for a monatomic chain

Let x_n be the position of the n-th atom, which in equilibrium has have $x_n^{(\mathrm{eq})} = na$. Then,

$$\delta x_n = x_n - x_n^{(\mathrm{eq})} \tag{3.1}$$

Using NII on x_n, we can write its equation of motion as

$$m\,\delta\ddot{x}_n = \kappa(\delta x_{n+1} - \delta x_n) - \kappa(\delta x_n - \delta x_{n-1}) = \kappa(\delta x_{n+1} + \delta x_{n-1} - 2\delta x_n) \tag{3.2}$$

where a dot denotes a derivative with respect to time. Our system is clearly periodic in a in real space, meaning that our wave-like solution must also be periodic in $2\pi/a$ in k-space. We thus consider a solution of the form

$$\delta x_n = Ae^{i(\omega t - kna)} \tag{3.3}$$

It is easy to verify that this is indeed invariant under the transformation $k \mapsto k + 2\pi/a$.

Dispersion Relation

Substituting the solution into (3.2), it follows quickly that the dispersion relation for the monatomic chain is given by

$$\boxed{\omega = 2\omega_0 \left|\sin\frac{ka}{2}\right|, \quad \omega_0 = \sqrt{\frac{\kappa}{m}}} \tag{3.4}$$

Once again, we observe that this is $2\pi/a$ periodic in k-space, meaning that the first Brillouin zone has boundaries $[-\pi/a, \pi/a]$. By definition, all physically distinct states of the system must be contained within this range, and so the dispersion relation and any quantities derived from it must have this periodicity.

We can calculate the number of states contained in the first Brillouin zone. Recalling that there are N masses in our chain, we impose the periodic boundary condition $\delta x_n = \delta x_{n+N}$ on our solution:

$$e^{i(\omega t - kna)} = e^{i(\omega t - k(N+n)a)} \quad \longrightarrow \quad e^{ikNa} = 1, \quad k = \frac{2\pi p}{Na} \tag{3.5}$$

where p is an integer. These are the possible allowed modes in k. The total number of modes in the first Brillouin zone is given by

$$\text{Total \# of modes} = \frac{\text{Range of } k}{\text{Spacing between discrete } k} = \frac{2\pi/a}{2\pi/Na} = N \tag{3.6}$$

However, as the Brillouin zone contains all physically distinct states, we must conclude that there are N different normal modes for a system of N masses.

It is easy to show from (3.4) that the phase and group velocities are given by

$$v_p = \frac{\omega}{k} = \frac{2\omega_0}{k}\left|\sin\frac{ka}{2}\right|, \quad v_g = \frac{d\omega}{dk} = a\omega_0\left|\cos\frac{ka}{2}\right| \tag{3.7}$$

The second of these follows most easily by differentiating ω^2, instead of ω. Note that by definition, the group velocity on any Brillouin zone boundary is zero. These are graphed in figures 3.2 and 3.3.

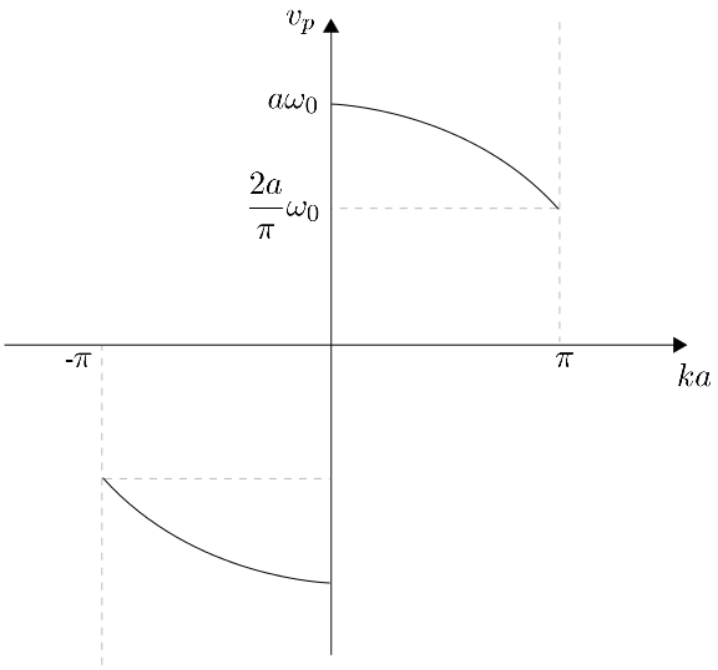

Figure 3.2: The phase velocity of a monatomic chain

Sound waves

Sound waves are vibrations that have a long wavelength in comparison to the inter-atomic spacing. This means that the sound velocity is given by

$$c_s = \lim_{k\to 0} v_g = a\omega_0 = a\sqrt{\frac{\kappa}{m}} \tag{3.8}$$

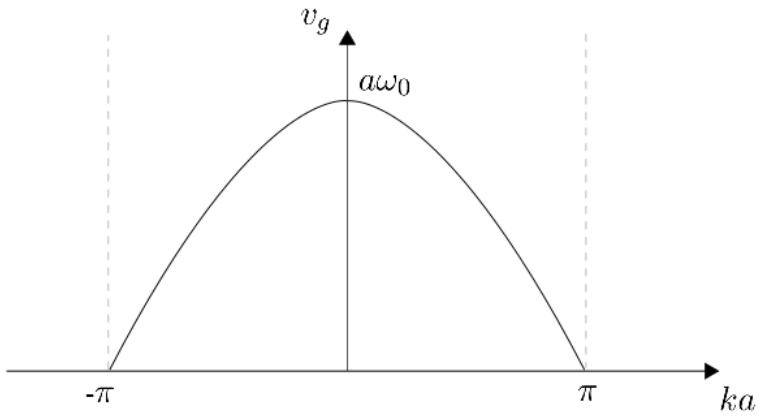

Figure 3.3: The group velocity of a monatomic chain

We note that the density of the unit cell is $\rho = m/a$, while the compressibility is $\beta_s = 1/\kappa a$, meaning that we can in fact write the sound velocity as

$$c_s = a\sqrt{\frac{1/(\beta_s a)}{\rho a}} = \frac{1}{\sqrt{\rho\beta_s}} \tag{3.9}$$

In fact, this relationship is true in general. Consider the definition of compressibility (1.21), and assume that $\rho = N/V$ for some number of atoms N. Then:

$$\beta_s = -\frac{1}{V}\frac{\partial V}{\partial p} = -\rho\frac{\partial}{\partial p}\left(\frac{1}{\rho}\right) = -\rho\frac{\partial}{\partial \rho}\left(\frac{1}{\rho}\right)\frac{\partial \rho}{\partial p} \tag{3.10}$$

By noticing that

$$c_s^2 = \frac{\partial \rho}{\partial p}, \quad \frac{\partial}{\partial \rho}\left(\frac{1}{\rho}\right) = -\frac{1}{\rho^2} \tag{3.11}$$

the general relationship in (3.9) follows.

Energy and Heat Capacity

Let us now consider the internal energy and heat capacity of our chain. For this, we need to calculate the density of states. We have two modes of 'polarisation' for the oscillations (backwards and forwards along the chain), meaning that we can write

$$g(k)dk = 2\frac{L}{2\pi}dk = \frac{Na}{\pi}dk \tag{3.12}$$

where we have made use of the fact that our system size is $L = Na$. We can write this in terms of the frequency as

$$g(\omega)d\omega = \frac{Na}{\pi}\left|\frac{dk}{d\omega}\right|d\omega = \frac{Na}{\pi}\frac{d\omega}{|v_g|} \tag{3.13}$$

Recognising that

$$\cos^2\frac{ka}{2} = 1 - \sin^2\frac{ka}{2} = 1 - \left(\frac{\omega}{2\omega_0}\right)^2 \tag{3.14}$$

it is clear that the density of states per angular frequency can be written as

$$\boxed{g(\omega) = \frac{2N}{\pi}\frac{1}{\sqrt{\omega_m^2 - \omega^2}}, \quad \omega_m = 2\omega_0} \tag{3.15}$$

We now assume that the classical vibrations of our monatomic chain can be modelled as lattice phonons that obey Bose-Einstein statistics. Then, we can write the energy as

$$U = \int d\omega\, \bar{n}_i g(\omega) \hbar\omega = \frac{2N}{\pi} \int_0^{\omega_m} d\omega\, \frac{1}{\sqrt{\omega_m^2 - \omega^2}} \frac{\hbar\omega}{e^{\beta\hbar\omega} - 1} \tag{3.16}$$

The heat capacity is given by

$$C_V = \frac{\partial U}{\partial T} = -\frac{\beta}{T}\frac{\partial U}{\partial \beta} = \frac{\beta}{T}\frac{2N}{\pi} \int_0^{\omega_m} d\omega\, \frac{(\hbar\omega)^2}{\sqrt{\omega_m^2 - \omega^2}} \frac{e^{\beta\hbar\omega}}{(e^{\beta\hbar\omega} - 1)^2} \tag{3.17}$$

We can non-dimensionalise this integral using the usual substitution $x = \beta\hbar\omega$, such that

$$C_V = \frac{2Nk_B}{\pi} \int_0^{x_m} dx\, \frac{1}{\sqrt{x_m^2 - x^2}} \frac{x^2 e^x}{(e^x - 1)^2} \tag{3.18}$$

In the high temperature limit, $x, x_m \ll 1$ meaning that the second fraction in the integrand becomes approximately unity. This means that the heat capacity becomes $C_V = Nk_B = R$, which is the law of Dulong-Petit in one dimension.

3.1.2 Diatomic Chain

Let us now generalise the previous discussion above to systems containing more than one type of atom. We shall consider the case where have a one-dimensional chain of N unit cells of length a, containing two atoms of masses m_1 and m_2, connected by a classical spring of spring constant κ. We shall label the atoms of mass m_1 by the positions x_n and the atoms of mass m_2 by y_n, as shown in figure 3.4 below.

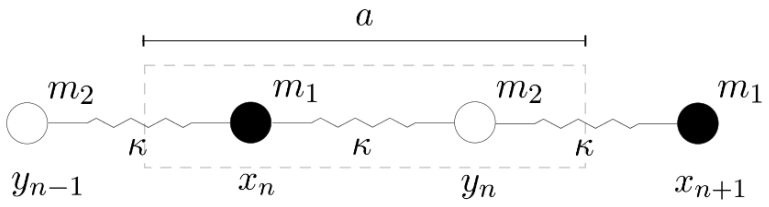

Figure 3.4: A schematic diagram for a diatomic chain

As before, we can use NII to find the equations of motion for both species of masses:

$$m_1\, \delta\ddot{x}_n = \kappa(\delta y_{n-1} - \delta x_n) - \kappa(\delta x_n - \delta y_n) = \kappa(\delta y_{n-1} + \delta y_n - 2\delta x_n) \tag{3.19}$$

$$m_2\, \delta\ddot{y}_n = \kappa(\delta x_{n+1} - \delta y_n) - \kappa(\delta y_n - \delta x_n) = \kappa(\delta x_{n+1} + \delta x_n - \delta 2y_n) \tag{3.20}$$

As before, we suppose that we have wave-like solutions of the form

$$\delta x_n = A_x e^{i(\omega t - kna)} \tag{3.21}$$

$$\delta y_n = A_y e^{i(\omega t - kna)} \tag{3.22}$$

Note that we have not assumed that the amplitudes of oscillation for each species is the same (as it is indeed not). Substituting these solutions into the equations of motion yields a matrix equation

$$\begin{pmatrix} 2\kappa - m_1\omega^2 & -\kappa\left(1 + e^{ika}\right) \\ -\kappa\left(1 + e^{-ika}\right) & 2\kappa - m_2\omega^2 \end{pmatrix} \begin{pmatrix} A_x \\ A_y \end{pmatrix} = 0 \tag{3.23}$$

For a solution to exist, we require that the determinant of the coefficient matrix is zero. Performing this calculation gives the dispersion relation

$$\boxed{\omega_\pm^2 = \kappa\left(\frac{1}{m_1} + \frac{1}{m_2}\right) \pm \kappa\left(\frac{1}{m_1^2} + \frac{1}{m_2^2} + \frac{2}{m_1 m_2}\cos ka\right)^{1/2}} \tag{3.24}$$

Optical and Acoustic Modes

It will not have escaped the readers attention that we have two modes of oscillation for each value of k, meaning that we have $2N$ normal modes for N unit cells. These modes are known as

- Acoustic - This is any mode that has linear dispersion as $k \to 0$, corresponding to sound waves. In acoustic modes, the masses oscillate together in the long wavelength limit, corresponding to the eigenvector $(A_x, A_y) = (1, 1)$ in (3.23) evaluated at $k = 0$. Examining the limit of $k = 0$ in the dispersion relation makes it clear that the acoustic modes correspond to ω_-
- Optical - This is any mode that has constant dispersion as $k \to 0$, so called because these phonons have non-zero energy at $k = 0$, and so can interact with light. In optical modes, the masses oscillate in anti-phase, corresponding to the eigenvector $(A_x, A_y) = (1, -1)$ in (3.23) evaluated at $k = 0$. This means that they are usually higher in energy than the acoustic modes. The optical modes clearly correspond to ω_+.

In general in one dimension, if we have M atoms per unit cell, there will be one acoustic mode and $M - 1$ optical modes. Then, the number of modes in the first Brillouin zone will be given by $2MN$. In three dimensions, we will have 3 acoustic, and $3M - 3$ optical modes. Introducing $\mu = m_1 m_2/(m_1 + m_2)$ and $M = m_1 + m_2$, we can write the dispersion relation as

$$\omega_\pm^2 = \frac{\kappa}{\mu}\left[1 \pm \left(1 - \frac{4\mu}{M}\sin^2\frac{ka}{2}\right)^{1/2}\right] \tag{3.25}$$

which allows us to find the values of the frequency at $k = 0$ and at the Brillouin zone boundary ($k = \pi/a$). In particular, let us consider the sound speed. Expanding $\sin x \approx x$, $(1 - x)^{1/2} \approx 1 - x/2$, we have that

$$\omega_-^2 \approx \frac{\kappa}{\mu}\left[1 - \left(1 - \frac{2\mu}{M}\left(\frac{ka}{2}\right)^2\right)\right] = \frac{\kappa}{2M}a^2k^2 \tag{3.26}$$

Thus, the sound velocity is given by

$$c_s = \frac{d\omega_-}{dk} = a\sqrt{\frac{\kappa}{2(m_1 + m_2)}} \tag{3.27}$$

We note that the density of the unit cell is $\rho = (m_1 + m_2)/a$, and that the effective spring constant is $\kappa/2$, meaning that $\beta_s = 2/a\kappa$. We can thus explicitly verify that (3.27) obeys the general relationship (3.9).

Reduced and Extended Zone Schemes

We can plot the dispersion relation (3.24) in two ways. The *reduced zone scheme* plots both solutions ontop of one another in the first Brillouin zone, as shown in figure 3.5. However, as the dispersion relation is once again periodic under the transformation $k \mapsto k + 2\pi/a$, we can plot one of the modes (usually the optical modes) in the second Brillouin zone $\pm[\pi/a, 2\pi/a]$. One can think of this as 'unfolding' the dispersions such that there is only one mode at each value of k, though of course k's that are distant from one another by $2\pi/a$ (the reciprocal lattice vector for our system) are entirely physically equivalent. This is known as the *extended zone scheme*, as shown in 3.6.

One immediate thing to notice about both of these plots is that there is an energy gap between each of these modes, behaviour that will become more important in later considerations. As $m_1 \to m_2$, the branches of the extended zone scheme will approach one another until they meet for $m_1 = m_2$. At this value, we obtain the same equations for a monatomic chain, except with $ka \mapsto ka/2$ as we have doubled the zone of the Brillouin zone in the diatomic case.

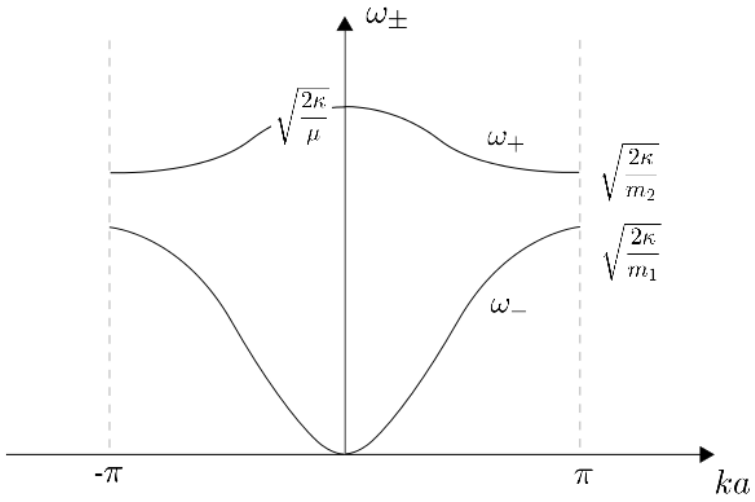

Figure 3.5: The diatomic chain dispersion relation in the reduced zone scheme ($m_2 < m_1$)

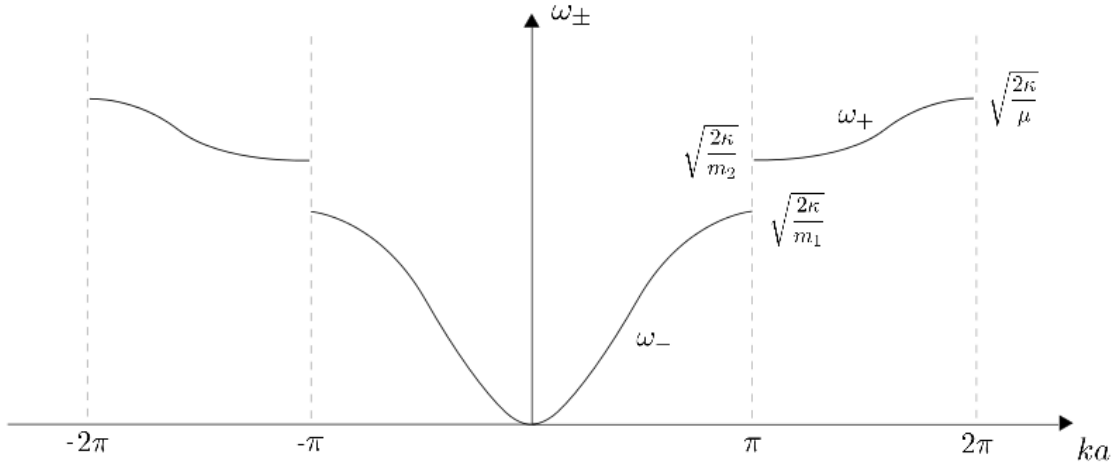

Figure 3.6: The diatomic chain dispersion relation in the extended zone scheme ($m_2 < m_1$)

3.2 Electrons in a Periodic Potential

Let us now consider how electrons behave within solids. Evidently, these electrons will be under the influence of the very complicated potential that results from the atoms within the lattice. However, we note that this potential must be periodic, repeating for each unit cell. This simplifies the situation significantly, as we now only have to consider the potential due to the atoms within the unit cell. We shall consider two models at opposite extremes; one where the electrons are tightly bound to their atoms, and one where they are able to propagate throughout the lattice as free particles. We shall see that both of these models give qualitatively the same results, meaning that we can assume that the electrons in solids do indeed behave in a similar way.

3.2.1 Bloch's Theorem

Suppose that we can describe electrons by the Hamiltonian

$$H = \frac{\mathbf{p}^2}{2m} + V(\mathbf{r}) \tag{3.28}$$

where the potential is periodic under translations by the direct lattice vector $\mathbf{R}$, meaning that it satisfies

$$V(\mathbf{r}) = \mathbf{V}(\mathbf{r} + \mathbf{R}) \tag{3.29}$$

Then, the Time Independent Schrödinger equation for this system in the position representation

$$\left[\frac{\mathbf{p}^2}{2m} + V(\mathbf{r})\right]\psi(\mathbf{r}) = E\psi(\mathbf{r}) \tag{3.30}$$

We can Fourier transform this equation into reciprocal space, yielding

$$\sum_{\mathbf{k}'} V_{\mathbf{k}-\mathbf{k}'}\psi_{\mathbf{k}'} = \sum_{\mathbf{G}} V_{\mathbf{G}}\psi_{\mathbf{k}-\mathbf{G}} = \left[E - \frac{\hbar^2|\mathbf{k}|^2}{2m}\right]\psi_{\mathbf{k}} \tag{3.31}$$

where we have used the fact that $V_{\mathbf{k}-\mathbf{k}'}$ is only nonzero for $\mathbf{k} - \mathbf{k}' = \mathbf{G}$. This means that for each value of $\mathbf{k}$, we can solve the Schrödinger equation for the set of $\psi_{\mathbf{k}-\mathbf{G}}$'s, for which we obtain solutions of the form

$$\boxed{\psi^{\alpha}_{\mathbf{k}}(\mathbf{r}) = \sum_{\mathbf{G}} u^{\alpha}_{\mathbf{G},\mathbf{k}}(\mathbf{r})e^{i(\mathbf{G}+\mathbf{k})\cdot\mathbf{r}}} \tag{3.32}$$

This is a statement of *Bloch's theorem*; the wavefunction of an electron can be decomposed in terms of crystal momentum $\mathbf{k}$, where $u^{\alpha}_{\mathbf{G},\mathbf{k}}(\mathbf{r})$ is periodic in the unit cell, and the values of $\mathbf{k}$ can be chosen within the first Brillouin zone. In the reduced zone scheme, there may be many states at each value, which are indexed by α. This is essentially a statement of the conservation of crystal momentum. For us, it means that we can always look for wave-like solutions to problems involving periodic potentials (regardless of the strength of the potential), as this decomposition will always remain valid.

3.2.2 The Tight-Binding Model

Consider a series of N adjacent atoms with a single electronic orbital, and spaced by a. Let $|n\rangle$ be the state corresponding to an electron being bound in the orbital of the n-th atom. Suppose that the a priori energy to occupy this state is E_0, while the energy gain associated with 'hopping' to adjacent sites $|n+1\rangle$ and $|n-1\rangle$ is $-t$. The negative sign

arises due to the fact that the electron has lower energy when confined to a larger area (more orbitals). We thus want to find some Hamiltonian that satisfies

$$\langle n| H |n\rangle = E_0 \tag{3.33}$$
$$\langle n \pm 1| H |n\rangle = -t \tag{3.34}$$

We now assume that all of the states $|n\rangle$ are orthogonal, which corresponds to the electrons being very tightly bound to the atoms, such that it has a very low probability of being on any other site. With this assumption, it is clear that the correct Hamiltonian is given by

$$\boxed{H = \sum_n \left[(E_0 |n\rangle \langle n|) - t \left(|n\rangle \langle n-1| + |n\rangle \langle n+1| \right) \right]} \tag{3.35}$$

where the sum n runs over all of the atoms N. We can now look for solutions to the Time Independent Schrödinger equation that are a superposition of all the possible orbital states:

$$|\psi\rangle = \sum_n \phi_n |n\rangle \tag{3.36}$$

Then:

$$\sum_n \left(E_0 \phi_n - t\phi_{n-1} - t\phi_{n+1} \right) |n\rangle = E \sum_n \phi_n |n\rangle \tag{3.37}$$

As the states $|n\rangle$ are orthogonal, we can drop the summation notation, such that our equation becomes:

$$E_0 \phi_n - t\phi_{n-1} - t\phi_{n+1} = E\phi_n \tag{3.38}$$

Motivated by Bloch's theorem, let us use the wave ansatz

$$\phi_n = e^{i(\omega t - kna)} \tag{3.39}$$

which upon substitution gives the dispersion relation

$$\boxed{E(k) = E_0 - 2t\cos(ka)} \tag{3.40}$$

Like in the case of the atomic chain model, the dispersion is periodic, and the Brillouin zone is of the same width $2\pi/a$. Furthermore, this dispersion relation gives rise to an *energy band* that comprises of the possible energy states at a given k, dictated by the amount of orbital overlap (hopping). The width of this energy band (the *bandwidth*) is $4t$.

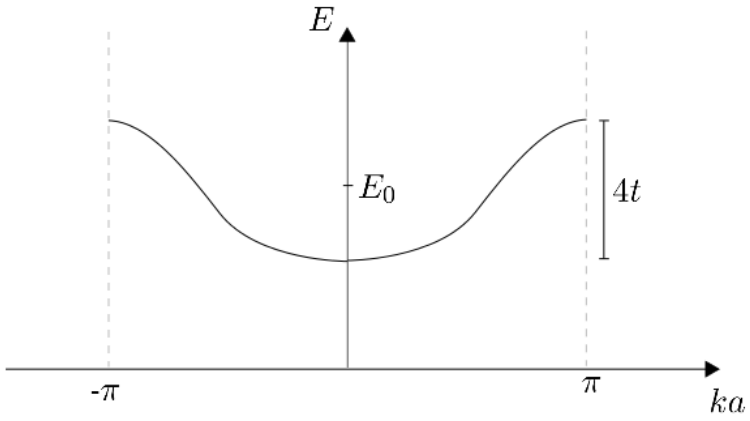

Figure 3.7: Energy dispersion for the tight-binding model with a single orbital per site

Around the bottom of the band ($k \to 0$), we have that

$$E(k) = \text{constant} + ta^2k^2 \tag{3.41}$$

We can thus view the electrons towards the bottom band as being free by defining an *effective mass* m^*:

$$\frac{h^2k^2}{2m^*} = ta^2k^2 \quad \longrightarrow \quad m^* = \frac{\hbar^2}{2ta^2} \tag{3.42}$$

This is the mass that the electron would effectively have if it was free, but with the same energy.

Lastly, let us calculate the internal energy and heat capacity for this model. The density of states is given by

$$g(k)dk = 2(2s+1)\frac{L}{2\pi}dk \tag{3.43}$$

where s is the spin of the system, and the extra factor of two comes from the fact that the integral is actually over the entire range $[-\infty, \infty]$, but we shall only be considering positive k's. In terms of energy, the density of states becomes

$$g(E)dE = 2(2s+1)\frac{L}{2\pi}\left|\frac{dk}{dE}\right|dE = \frac{(2s+1)N}{\pi\sqrt{(2t)^2 - (E_0 - E)^2}}dE \tag{3.44}$$

where we have used (3.40) and the fact that $L = Na$. Now electrons, $s = 1/2$, meaning that the density of states per unit energy for this single orbital tight binding model is

$$\boxed{g(E) = \frac{2N}{\pi\sqrt{(2t)^2 - (E - E_0)^2}}} \tag{3.45}$$

As we are considering electrons, the system will behave according to Fermi-Diract statistics. Letting $\widetilde{E} = E - E_0$, and $\widetilde{E}_m = 2t$, such that our integral for the energy is

$$U = \frac{2N}{\pi}\int_0^{\widetilde{E}_m} d\widetilde{E}\,\frac{1}{\sqrt{\widetilde{E}_m^2 - \widetilde{E}^2}}\,\frac{\widetilde{E}}{e^{\beta\widetilde{E}} - 1} \tag{3.46}$$

The heat capacity is then given by

$$C_V = \frac{\partial U}{\partial T} = -\frac{\beta}{T}\frac{\partial U}{\partial \beta} = \frac{2N\beta}{\pi T}\int_0^{\widetilde{E}_m} d\widetilde{E}\,\frac{\widetilde{E}^2}{\sqrt{\widetilde{E}_m^2 - \widetilde{E}^2}}\,\frac{e^{\beta\widetilde{E}}}{(e^{\beta\widetilde{E}} - 1)^2} \tag{3.47}$$

As before, we can non-dimensionalise this integral using $x = \beta\widetilde{E}$, such that

$$C_V = \frac{2Nk_B}{\pi}\int_0^{x_m} dx\,\frac{1}{\sqrt{x_m^2 - x^2}}\,\frac{x^2e^x}{(e^x - 1)^2} \tag{3.48}$$

We can evaluate this in the low temperature limit, for which $x, x_m \gg 1$. Then:

$$C_V \approx \frac{2Nk_B}{\pi}\frac{1}{x_m}\int_0^{\infty} dx\,x^2e^{-x} = \frac{2Nk_B}{\pi}\frac{k_BT}{2t} \tag{3.49}$$

Thus, the heat capacity is linear in the low-temperature limit, which agrees with the predictions of the Sommerfeld model. This is somewhat perplexing; the Sommerfeld model was for a free electron gas, while this is the case where electrons are tightly bound to atoms.

Two Orbitals

We now consider the case where each site has two atomic orbitals A and B. This can also be though of modifying the unit cell of the system to contain two atoms (diatomic). In our Hamiltonian, we need to take account of the fact that the electron can hop between the two orbitals on the given site, as well as to either of the orbitals on adjacent sites. By inspection, the Hamiltonian in this case is

$$H = \sum_n \left[(E_0^A |A_n\rangle \langle A_n|) + (E_0^B |B_n\rangle \langle B_n|) - t(|A_n\rangle \langle B_n| + |B_n\rangle \langle A_{n-1}|) \right. \\ \left. -t(|B_n\rangle \langle A_n| + |A_n\rangle \langle B_{n-1}|) \right] \tag{3.50}$$

As before, we look for solutions of the form

$$|\psi\rangle = \sum_n \phi_n^A |A_n\rangle + \phi_n^B |B_n\rangle \tag{3.51}$$

which yields - again assuming that the states are orthogonal, allowing us to drop the summation notation - the following coupled differential equations:

$$E\phi_n^A = E_0^A \phi_n^A - t(\phi_n^B + \phi_{n-1}^B) \tag{3.52}$$

$$E\phi_n^B = E_0^B \phi_n^B - t(\phi_n^A + \phi_{n-1}^A) \tag{3.53}$$

Again motivated by Bloch's theorem, we adopt the wave ansatz

$$\phi_n^A = Ae^{i(\omega t - kna)} \tag{3.54}$$

$$\phi_n^B = Be^{i(\omega t - kna)} \tag{3.55}$$

Substituting these solutions into the coupled differential equations yields the matrix equation:

$$\begin{pmatrix} E_0^A - E & -t\left(1 + e^{ika}\right) \\ -t\left(1 + e^{ika}\right) & E_0^B - E \end{pmatrix} \begin{pmatrix} A \\ B \end{pmatrix} = 0 \tag{3.56}$$

In order for a solution to exist, the determinant of the coefficient matrix must be zero. Performing this calculation yields the dispersion relation

$$E_\pm(k) = \frac{1}{2}\left[E_0^A + E_0^B \pm \left(\left(E_0^A - E_0^B\right)^2 + 8t^2(1 + \cos ka) \right)^{1/2} \right] \tag{3.57}$$

In the limit that $t \to 0$ (corresponding to even tighter binding), the energy spectrum becomes constant, as we re-obtain the possible energy eigenvalues E_0^A and E_0^B for the two orbitals. This dispersion is plotted in the extended zone scheme in figure 3.8 below.

We again have discrete energy bands, but now they are separated by an energy gap known as the *band gap*. The gap is dependent on the magnitude t; the greater its value, the larger the band gap. This corresponds to the electrons being less tightly bound to the atoms. We shall examine the significance of band gap more closely in section 3.3.

We can also find an effective mass for electrons in the lower band around $k = 0$ by expanding the square root as

$$\left(\left(E_0^A - E_0^B\right)^2 + 8t^2(1 + \cos ka) \right)^{1/2} \approx \left(\left(E_0^A - E_0^B\right)^2 + 16t^2 - 4(tka)^2 \right)^{1/2} \\ \approx \left(\left(E_0^A - E_0^B\right)^2 + 16t^2 \right) \left(1 - \frac{4(tka)^2}{\left(E_0^A - E_0^B\right)^2 + 16t^2} \right) \tag{3.58}$$

The rest has been left as an exercise to the reader. However, it is clear that this will reduce nicely to (3.42) (up to factors of order unity) in the limit that $E_0^A = E_0^B$.

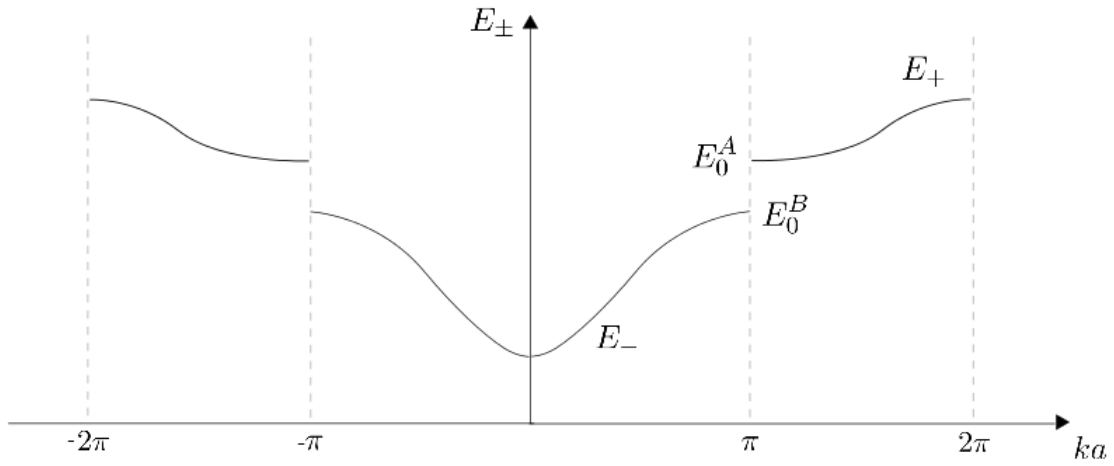

Figure 3.8: Energy dispersion for the tight-binding model with two orbitals per site ($E_0^B < E_0^A$)

3.2.3 The Nearly-Free Electron Model

As the same suggests, we are now going to look at the other extreme in which the electrons are free to move throughout our lattice, but subject to some weak periodic potential $V(\mathbf{r})$, such that the Hamiltonian of the system becomes:

$$H = \frac{\mathbf{p}^2}{2m} + V(\mathbf{r}), \quad V(\mathbf{r}) = V(\mathbf{r}+\mathbf{R}) \tag{3.59}$$

Suppose that we initially have an incident plane wave of the form $\langle \mathbf{r}|\mathbf{k}\rangle = Ae^{i\mathbf{k}\cdot\mathbf{x}}$ for some wavevector $\mathbf{k}$. This will be scattered by the weak potential to give a wave of the form $\langle \mathbf{r}|\mathbf{k}'\rangle = Be^{i\mathbf{k}'\cdot\mathbf{x}}$. We can decompose our potential as

$$V(\mathbf{r}) = \sum_{\mathbf{G}} e^{i\mathbf{G}\cdot\mathbf{r}} V_{\mathbf{G}} = \sum_{\mathbf{G}} e^{i\mathbf{G}\cdot(\mathbf{r}+\mathbf{R})} V_{\mathbf{G}} \tag{3.60}$$

In order for the terms in this sum to be non-zero, we require that the Laue condition is satisfied, meaning that $\mathbf{k}' = \mathbf{k} + \mathbf{G}$. Thus, we can write the state of the system (in the position representation) as:

$$\langle \mathbf{r}|\psi\rangle = Ae^{i\mathbf{k}\cdot\mathbf{r}} + Be^{i(\mathbf{k}+\mathbf{G})\cdot\mathbf{r}}, \quad |\psi\rangle = |\mathbf{k}\rangle + \left|\mathbf{k}'\right\rangle \tag{3.61}$$

By (1.6), we want to calculate the matrix elements for our Hamiltonian. We define the matrix elements

$$\langle \mathbf{k}| H |\mathbf{k}\rangle = E_0(\mathbf{k}) + V_0 \tag{3.62}$$
$$\left\langle \mathbf{k}'\right| H \left|\mathbf{k}'\right\rangle = E_0(\mathbf{k}') + V_0 \tag{3.63}$$
$$\langle \mathbf{k}| H \left|\mathbf{k}'\right\rangle = V_{\mathbf{k}-\mathbf{k}'} = V_{-\mathbf{G}} = V_{\mathbf{G}}^* \tag{3.64}$$

meaning that our effective Schrödinger equation becomes:

$$\begin{pmatrix} E_0(\mathbf{k}) + V_0 - E & V_G \\ V_G^* & E_0(\mathbf{k}') + V_0 - E \end{pmatrix} \begin{pmatrix} A \\ B \end{pmatrix} = 0 \tag{3.65}$$

We shall now consider two particular cases of this expression, as the general case is not particularly interesting or informative. Arguably, none of this is neither interesting nor informative; such is Condensed Matter Physics at an undergraduate level.

At the Brillouin Zone Boundary

Suppose that we are on the Brillouin zone boundary. Then, $\mathbf{k} = \mathbf{k}'$, meaning that we can solve (3.65) very simply to yield

$$\boxed{E_{\pm}(\mathbf{k}) = \frac{\hbar^2|\mathbf{k}|^2}{2m} + V_0 \pm |V_{\mathbf{G}}|} \tag{3.66}$$

where we have used the fact that $\mathbf{E}_0(\mathbf{k})$ is the expectation value of the kinetic energy. This is graphed (in one dimension) in figure 3.9 below.

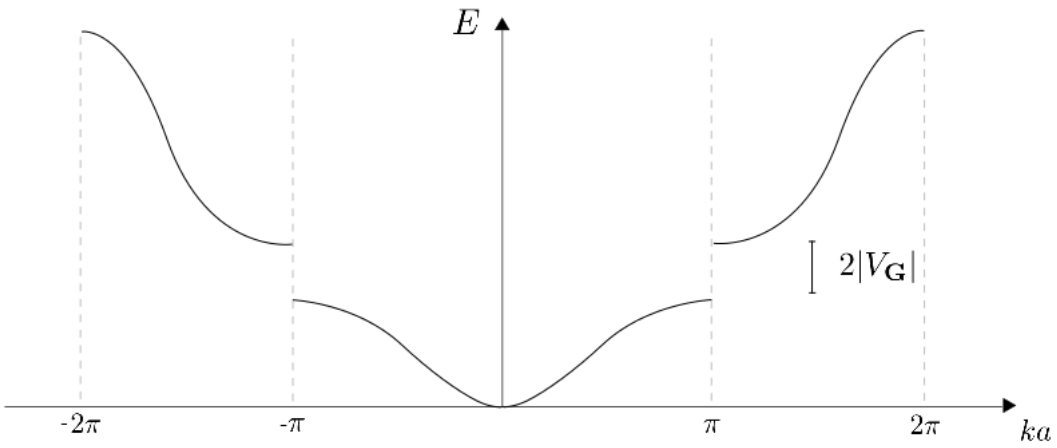

Figure 3.9: Energy dispersion for the nearly free electron model on the Brillouin zone boundary

Once again, the energy is organised into bands, with a band-gap $2|V_{\mathbf{G}}|$. What is the condition for this gap to exist? In general, we require that the highest energy in the lower band to be smaller than the lowest energy in the upper band. In this case, we shall say that the potential needs to be on the order of the kinetic energy at the Brillouin zone boundary, namely that

$$|V_{\mathbf{G}}| \approx \frac{\hbar^2|\mathbf{k}|^2}{2m} \tag{3.67}$$

We can also gain an understanding of how this band-gap originates. The two eigenstates of the system (in the position representation) are

$$\langle \mathbf{r}|\mathbf{k}\rangle_{\pm} = \frac{1}{\sqrt{2}}\left[\langle \mathbf{r}|\mathbf{k}\rangle \pm \langle \mathbf{r}|\mathbf{k}'\rangle\right] \tag{3.68}$$

Suppose that we are in the one-dimensional potential $V(x) = V_0 + V_G\cos(2\pi x/a)$. Then, the eigenstates become

$$\langle x|k\rangle_{+} \propto \cos\frac{\pi x}{a}, \quad \langle x|k\rangle_{-} \propto \sin\frac{\pi x}{a} \tag{3.69}$$

Considering the probability densities $\left|\langle x|k\rangle_{\pm}\right|^2$ of both eigenstates, it is clear that $\langle x|k\rangle_{+}$ has its probability density concentrated at the maxima of $V(x)$, where as $\langle x|k\rangle_{-}$ has its density concentrated at the minima of $V(x)$. This gives rise to an energy difference between the two states, as it raises the energy of one by V_G and lowers the energy of the other by V_G.

Near the Brillouin Zone Boundary

We shall treat this situation in one-dimension. Near the Brillouin zone boundary, we let the kinetic energies be

$$E_0(k+\delta k) = \frac{\hbar^2}{2m}\left[\left(\frac{n\pi}{a}\right)^2 + \frac{2n\pi}{a}\delta k + \delta k^2\right] \tag{3.70}$$

$$E_0(k'+\delta k) = \frac{\hbar^2}{2m}\left[\left(\frac{n\pi}{a}\right)^2 - \frac{2n\pi}{a}\delta k + \delta k^2\right] \tag{3.71}$$

where we have let $k = n\pi/a$ and $k' = -n\pi/a$ for some integer n. From (3.65), we have the eigenvalue problem

$$\left(E_0(k) - E\right)\left(E_0(k') - E\right) - |V_G|^2 = 0 \tag{3.72}$$

Substituting the above relationships in, we find that

$$E_\pm = \frac{\hbar^2}{2m}\left[\left(\frac{n\pi}{a}\right)^2 + \delta k^2\right] \pm |V_G|\left[1 + \left(\frac{\hbar^2}{2m}\frac{2n\pi}{a}\frac{\delta k}{|V_G|}\right)^2\right]^{1/2} \tag{3.73}$$

We can now expand for $\delta k \ll k = n\pi/a$, $\delta k \ll |V_G|$, such that

$$E_\pm = E_\pm(\delta k = 0) + \frac{\hbar^2 \delta k^2}{2m}\left[1 \pm \frac{\hbar^2 (n\pi/a)^2}{m|V_G|}\right] \tag{3.74}$$

where $E_\pm(\delta k = 0)$ is simply the energy corresponding to being exactly on the Brillouin zone boundary, as given by (3.66). This can also be written as

$$E_\pm = E_\pm(\delta k = 0) + \frac{\hbar^2 \delta k^2}{2m^*_\pm} \tag{3.75}$$

where we have defined the effective masses

$$m^*_\pm = \frac{m}{\left[1 \pm \frac{\hbar^2 (n\pi/a)^2}{m|V_G|}\right]} \tag{3.76}$$

It is clear that the nearly free electron model predicts very similar behaviour to the tight-binding model in terms of the energy dispersion; they predict the formation of discrete energy bands, and the associated band gaps, when electrons are exposed to a periodic potential. As such, we are inclined to think that real lattices - that can be characterised by a periodic potential - also exhibit this behaviour.

3.3 Band Theory and Semiconductors

Suppose that there are N primitive unit cells in a crystal, and that the electron dispersion relation displays a band structure (meaning that there are discrete energy bands in which electronic states exist, separated by band gaps). How do the electrons fill these energy bands? We know that in each Brillouin zone, there are N possible states for the electrons. Due to Pauli exclusion, only two electrons can occupy each state, meaning that it takes $2N$ electrons to fill an entire band. In general, lattices with an even number of electrons per unit cell will have full bands, while those with an odd number will have at least one unfilled band.

We can apply this to our atomic chain models; the monatomic chain has half-filled bands if each atom is monovalent, but full bands if each atom is divalent. The diatomic chain has no choice but to have filled bands as the atoms are monovalent at the least. Similarly for the tight-binding model for both single and double orbitals.

The electrons within the filled band occupy all possible $\mathbf{k}$ states, meaning that there are no other states to move into within this band. This means that filled bands cannot cannot conduct, as they are not able to accept any more energy to move into another $\mathbf{k}$ state. In this case, the band also cannot contribute to the electronic heat capacity, as again the electrons cannot accept any more energy; the heat capacity thus becomes phonon dominated. We call the highest filled band the *valence band* and the empty band above this the *conduction band*, which are separated by an energy *band gap*. Evidently, partially filled bands are able to conduct.

3.3.1 Band Structure and the Fermi Surface

By definition, the Fermi surface is the surface corresponding to the maximum energy of the system at $T = 0$. This means that electrons will fill bands up to the Fermi surface. With this understanding, we can now classify materials into three groups:

- Conductors - These have at least one partially filled band. This may be a consequence of either having an odd number of valence electrons (monovalent), or because the energies of two adjacent bands overlap, meaning that parts of each lie beneath the Fermi surface such that they become partially filled
- Insulators - These have fully filled bands (even number of valence electrons, divalent), and the band gap energy is much greater than the thermal energy of the system, meaning that electrons cannot be excited into the conduction band. The Fermi surface for insulators usually sits between the valence and conduction bands
- Semiconductors - These have fully filled bands (even number of valence electrons, divalent), but the band gap energy is sufficiently small ($\lesssim 4\,\text{eV}$) that electrons can be thermally excited into the conduction band at finite temperatures. We shall examine these further in section 3.3.3

Note that it must be stressed that in the case of many atoms per unit cell, the total valence of all the atoms within the unit cell is the important number to consider in determining band structure. For example, SiC is made up of C : $[\text{He}]2s^2 2p^2$ and Si : $[\text{Ne}]3s^2 3p^2$, meaning that there are 8 valence electrons per unit cell, and 4 fully filled bands. However, SiC is a semiconductor as its band gap is quite small.

We can visualise the filling of bands in two-dimensions by sketching Fermi surfaces. In the absence of a periodic potential, the Fermi surface is simply a circle in $\mathbf{k}$-space, while here

we represent the first Brillouin zone as a square since we are restricting our consideration to square lattices. When the periodic potential is applied, states closer to the boundaries are shifted down in energy, deforming the Fermi surface. This is shown for monovalent atoms in figure 3.10. Note that in this case, the Fermi surface has an area half the size of the Brillouin zone, so it can fill - at maximum - half of the zone.

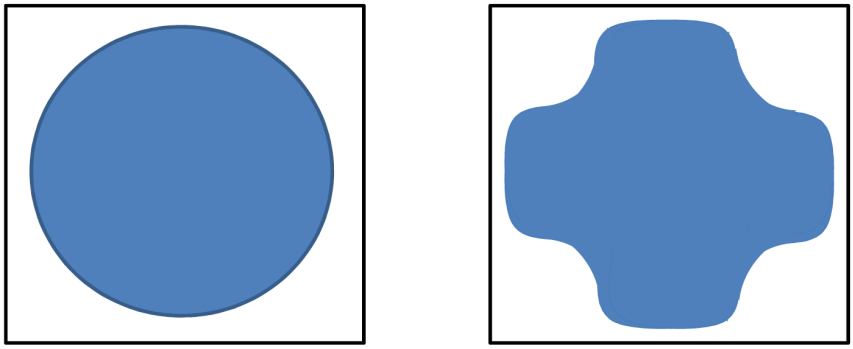

Figure 3.10: The Fermi surface for monovalent atoms in a square lattice in the absence of a potential (left), and with a potential (right)

For a divalent material, the circle has the same area as the Brillouin zone, and if the periodic potential is made sufficnetly strong, the states that originally like outside the first Brillouin zone are shifted up, and the ones inside are shifted down in energy, such that the entire Brillouin zone is occupied. This state corresponds to the system being an insulator.

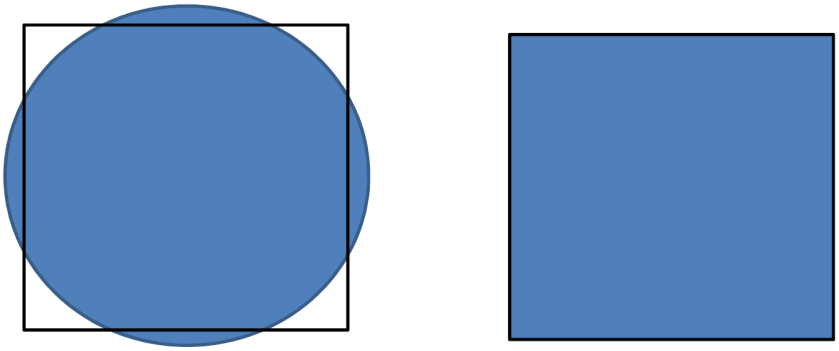

Figure 3.11: The Fermi surface for divalent atoms in a square lattice in the absence of a potential (left), and with a potential (right)

In the intermediate case, we observe the kind of deformation as in figure 3.12. There are some states in the first and second Brillouin zones, meaning that the system is still able to conduct. Note that the Fermi surface (under the application of a potential) must always intersect the Brillouin zone boundary at right angles, as the group velocity is zero here.

3.3.2 Optical Properties of Materials

We can also describe the optical properties of materials using band theory. The visible spectrum falls approximately in the range 1.65 eV to 3.2 eV, meaning that the maximum photon energy in the visible spectrum is $\hbar\omega \approx 3.2$ eV. This means that if a material has

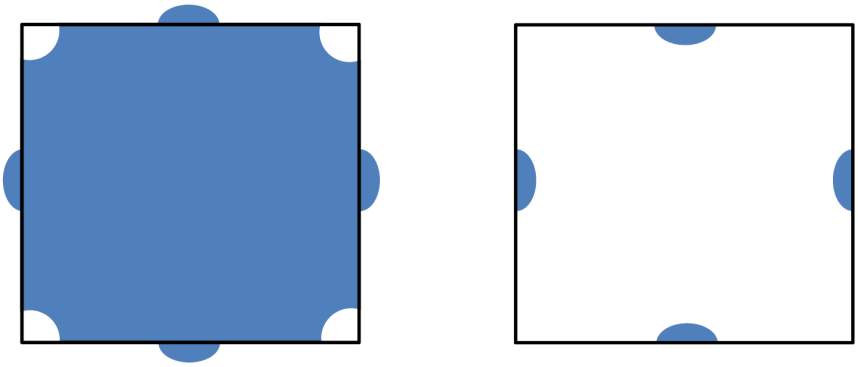

Figure 3.12: The Fermi surface for divalent atoms in a square lattice in the presence of a moderate potential. The left- and right-hand sides correspond to the extended and reduced zone schemes respectively

a band gap of more than this value, it appears transparent, since no single visible photon can cause excitation to the conduction band. This means that there is no scattering of electrons which causes opacity. This is the case with diamond, for example.

We also have to consider the way in which the electron transitions. *Direct transitions* between the valence and conduction bands do not change the value of $\mathbf{k}$, where as *indirect transitions* occur between the top of the valence band and the bottom of the conduction band, changing the value of $\mathbf{k}$. The minimum energy transition is an indirect one, by definition. However, photons alone cannot excite indirect transitions as momentum is not conserved. We still observe some electrons being excited in this way, as lattice phonons can re-distribute some of the momentum, but this is not a very dominant effect due to the poor coupling between photons and phonons.

Note that band theory completely ignores the Coulomb interaction between electrons, despite the fact that the associated energy can be greater than the Fermi energy. However, it turns out that it is fine to do this, for reasons that we shall not go into here. However, this does cause band theory to fail in describing Mott insulators, materials where the electron-electron repulsion is indeed a dominant effect, preventing our notional bands from filling up easily.

3.3.3 Semiconductor Physics

As they are the most physically intriguing out of insulators, conductors, and semiconductors, we shall examine further the physics of the latter. We will not be covering semiconducting devices, as these are non-examinable, and there are plenty of resources for further reading in this area if the reader so desires.

Electrons and Holes

The general picture of a semiconductor is a material with a mostly-full valence band, and a almost-empty conduction band, separated by a small band gap. As a result, it is convenient to define a *hole* as the absence of an electron in the valence band. This is a useful concept as we can characterise the motion of electrons in the conduction band as a flow of positively charged holes in the valence band, as the valence band is itself inert. This leads to the positively charged mass carriers that we mention in relation to the Hall effect. Note that we generally refer to the density of electrons as n and the density of holes as p.

We find the effective mass of the electrons by expanding the conduction band energy around its minimum value E_{min} at $\mathbf{k}_{\text{min}}$:

$$E = E_{\text{min}} + \alpha \left|\mathbf{k} - \mathbf{k}_{\text{min}}\right|^2 + \dots \tag{3.77}$$

We then define the *effective mass* $m*_e$ of the electron as satisfying

$$\boxed{\frac{\hbar^2}{m_e^*} = \frac{\partial^2 E}{\partial k^2} = 2\alpha} \tag{3.78}$$

where E is the electron dispersion relation. In an isotropic system, the derivative can be taken along any direction. For anisotropic system, the value of the effective mass should be evaluated along $\mathbf{e}_1$, $\mathbf{e}_2$ and $\mathbf{e}_3$, and then the overall effective mass can be calculated from

$$m^* = (m_{\mathbf{e}_1} m_{\mathbf{e}_2} m_{\mathbf{e}_3})^{1/2} \tag{3.79}$$

for density of states calculations. The corresponding group velocity is given by

$$\boxed{\mathbf{v}_e = \nabla_{\mathbf{k}} E/\hbar} \tag{3.80}$$

For holes, we expand the valence band energy around its maximum E_{max} at $\mathbf{k}_{\text{max}}$:

$$E = E_{\text{max}} - \alpha \left|\mathbf{k} - \mathbf{k}_{\text{max}}\right|^2 \tag{3.81}$$

We then always define the effective mass of the holes to be positive, meaning that

$$\boxed{\frac{\hbar^2}{m_h^*} = \left|\frac{\partial^2 E}{\partial k^2}\right| = 2\alpha} \tag{3.82}$$

Defining it in this way means that the energy required to move a hole away from $\mathbf{k}_{\text{min}}$ is positive, such that the minimum energy state is with the electron at the bottom of the conduction band, and the hole at the top of the valence band; the electron wants to sink, and the hole wants to rise. The energy of the hole is

$$E_h = \frac{\hbar^2 \left|\mathbf{k} - \mathbf{k}_{\text{max}}\right|^2}{2m_h^*} \tag{3.83}$$

with the corresponding group velocity being given by

$$\boxed{\mathbf{v}_p = \nabla_{\mathbf{k}} E_h/\hbar} \tag{3.84}$$

In the particular case of a filled band, overall crystal momentum must be conserved. This means that we can write that

$$\hbar\mathbf{k}_e + \hbar\mathbf{k}_h = 0 \quad \longrightarrow \quad \begin{cases} \mathbf{k}_e = -\mathbf{k}_h \\ |\mathbf{v}_e| = |\mathbf{v}_h| \end{cases} \tag{3.85}$$

By analogy to Drude theory, we can write the following transport equations for the electrons and holes:

$$m_e^* \frac{d\mathbf{v}_e}{dt} = -e(\mathbf{E} + \mathbf{v} \times \mathbf{B}) - \frac{m_e^* \mathbf{v}_e}{\tau_e} \tag{3.86}$$

$$m_h^* \frac{d\mathbf{v}_h}{dt} = \ \ e(\mathbf{E} + \mathbf{v} \times \mathbf{B}) - \frac{m_h^* \mathbf{v}_h}{\tau_h} \tag{3.87}$$

Note the charge of the holes. The scattering times allows us to define the *carrier mobility*

$$\mu_i = \frac{|\mathbf{v}_i|}{|\mathbf{E}|} = -\sigma_i R_{Hi} = \left|\frac{e\tau_i}{m_i^*}\right| \tag{3.88}$$

that measures how easily the electrons and holes (indexed by i) move. As indicated, we can determine carrier mobility from the Hall coefficient and conductivity of the given carrier.

Doping

In a pure or *intrinsic* semiconductor, the number density of electrons in the conduction band n and the number density of holes in the valence band p are the same. If, however, the semiconductor contains impurities, then it is said to be *doped*. There are two donor types:

- n-doped (donors) - A material with an extra electron is added to the lattice. The electrons from the donor atoms creates impurity eigenstates just below the empty conduction band, from where they can easily be excited into the conduction band. This shifts the chemical potential upwards (originally sitting midway in the bandgap at absolute zero, as we shall show). An example would be doping silicon with phosphorous
- p-doped (acceptors) - A material with one less electron is added to the lattice. The holes from the donor atoms create impurity eigenstates just above the valence band, into which electrons can be excited, and conduct. This shifts the chemical potential downwards. An example would be doping silicon with aluminium

When a material is doped, we can replace the mass of the charge carriers by their effective mass $m \mapsto m^*$. Furthermore, the material becomes polarisable, meaning that we replace $\epsilon_0 \mapsto \epsilon_0 \epsilon_r$. This allows us to define the effective Rydberg and Bohr radius

$$\mathcal{R}^{\text{eff}} = \mathcal{R}\left(\frac{m_e^*}{m}\frac{1}{\epsilon_r^2}\right), \quad a_0^{\text{eff}} = a_0\left(\frac{m_e}{m_e^*}\epsilon_r\right) \tag{3.89}$$

As typically $\epsilon_r \backsim 10$ and $m_e^* \backsim m_e/3$ for semiconductors, the effective electron binding energies are typically very small, while the effective radius is very large, on the scale of the unit cell. As such, we are justified in treating the carriers statistically (as we shall now do), as the thermal energies are dominant in comparison to the electronic energies of the system. Note that the fact that the effective Bohr radius is very large justifies our continuum treatment of the material; on small lengthscales, the electric field is incredibly inhomogeneous due to the atomic structure, but on large enough lengthscales, we can simply model the material as a medium with a constant dielectric constant.

The Law of Mass Action

Assuming that our system is isotropic, we can write the density of states for our system as

$$g(k)d^3\mathbf{k} = (2s+1)\frac{V}{(2\pi)^3}4\pi^2k^2dk = \frac{(2s+1)V}{2\pi^2}k^2dk \tag{3.90}$$

Adopting the usual free particle dispersion relation

$$E = \frac{\hbar^2k^2}{2m} \tag{3.91}$$

we can write our general density of states as

$$g(E)dE = \frac{(2s+1)Vm^{3/2}}{\sqrt{2}\pi^2\hbar^3}E^{1/2}dE \tag{3.92}$$

Now, in applying this to semiconductors, we need to take account of the fact that there is a bandgap. Electrons reside in the conduction band that has energy $E \geq E_c$ (where E_c is the minimum energy in the conduction band), while holes reside in the valence band that

has energy $E \leq E_v$ (where E_v is the maximum energy in the valence band). This means that we write the densities of states for each of the two charge carries as

$$g_c(E \geq E_c) = \frac{(2m_e^*)^{3/2}V}{2\pi^2\hbar^3}(E - E_c)^{1/2} \tag{3.93}$$

$$g_v(E \leq E_v) = \frac{(2m_h^*)^{3/2}V}{2\pi^2\hbar^3}(E_v - E)^{1/2} \tag{3.94}$$

As both electrons and holes are fermions ($s = 1/2$), we can describe their occupation numbers by Fermi-Dirac statistics

$$\bar{n}_i = \frac{1}{e^{\beta(E-\mu)} + 1} \approx e^{-\beta(E-\mu)} \tag{3.95}$$

where the last expression follows from assuming that the chemical potential is sufficiently far away from the conduction and valence bands that $\beta(E_g - \mu) \ll 1$, as is the case for almost all semiconductors. We can thus compute the number densities of the carriers. We shall do this for the electrons explicitly:

$$\begin{aligned} n = \frac{1}{V}\int dE\, g_c(E)\bar{n}_i &= \frac{(2m_e^*)^{3/2}}{2\pi^2\hbar^3}e^{\beta(\mu-E_c)}\int_{E_c}^{\infty} dE\,(E - E_c)^{1/2}e^{-\beta(E-E_c)} \\ &= \frac{(2m_e^* k_B T)^{3/2}}{2\pi^2\hbar^3}e^{\beta(\mu-E_c)}\underbrace{\int_0^{\infty} dx\, x^{1/2}e^{-x}}_{\sqrt{\pi}/2} \end{aligned} \tag{3.96}$$

where we have non-dimensionalised the integral using the substitution $x = \beta(E - E_c)$. Thus, we write the density of electrons as

$$n = \frac{1}{4}\left(\frac{2m_e^* k_B T}{\pi\hbar^2}\right)^{3/2} e^{-\beta(E_c-\mu)} \tag{3.97}$$

Similarly, the hole density can be found to be

$$p = \frac{1}{4}\left(\frac{2m_h^* k_B T}{\pi\hbar^2}\right)^{3/2} e^{-\beta(\mu-E_v)} \tag{3.98}$$

Their product is given by

$$\boxed{np = n_i^2 = \frac{1}{2}\left(\frac{k_B T}{\pi\hbar^2}\right)^3 (m_e^* m_h^*)^{3/2} e^{-\beta E_g}} \tag{3.99}$$

where $E_g = E_c - E_v$ is the band gap energy. This expression is sometimes known as *the law of mass action*, and is independent of doping material.

In intrinsic semiconductors, $n = p \equiv n_i$, making it easy to find the intrinsic carrier density from (3.99). Taking the ratio of (3.97) to (3.98), and re-arranging, we find that the chemical potential is given by

$$\mu = \frac{1}{2}(E_c + E_v) + \frac{3}{4}k_B T \log(m_h^*/m_e^*) \tag{3.100}$$

This means, as stated previously, that the chemical potential at absolute zero is midway between the bands. At finite temperatures, it moves towards the valence or conduction bands depending on the value of m_h^*/m_e^*. In general, $m_h^* > m_e^*$ as the upper band has greater curvature.

For doped semiconductors, the law of mass action still holes. In this case, it is often useful to define the *doping* D as

$$D = n - p = n_D - p_D \tag{3.101}$$

where n_D and p_D are the densities of donor and acceptor atoms respectively. The last equality holds by charge neutrality for the entire system. In n-type semiconductors, $p_D = 0$, and $n_i \ll n_D$, meaning that $n \backsim n_D$. Similarly, in p-type semiconductors, $n_D = 0$, and $p_i \ll p_D$, meaning that $p \backsim p_D$. Given D and n_i, we can solve (3.99) explicitly for n and p.

How does the total carrier density depend on temperature? At very low temperatures (large $1/T$), negligible intrinsic electron-hole pairs exist ($n_i \ll 1$), and the donor carriers become bound to their donor atoms ($D \backsim 0$). This is known as the *freeze-out* region. As the temperature is raised, increase ionisation occurs, and at about 100 K, all of the donor atoms are ionised, at which point the carrier concentration is dominated by doping ($n_i \ll D$) since thermal energies are still not high enough to create intrinsic electron-hole pairs. The region where every available dopant has been ionised is called the *extrinsic* region. In this region, an increase in temperature produces no increase in carrier concentration. Note that the horizontal value corresponding to the plateau gives the value of D. At even higher temperature, the thermal energies excite the large available population of intrinsic electron-hole pairs, such that $n_i \gg D$. This is the *intrinsic* region. Note that with the scales shown, we can calculate the band gap energy from the gradient of the line in the intrinsic region by using (3.99) for n_i:

$$\text{Gradient} = -\frac{E_g}{2k_B} \tag{3.102}$$

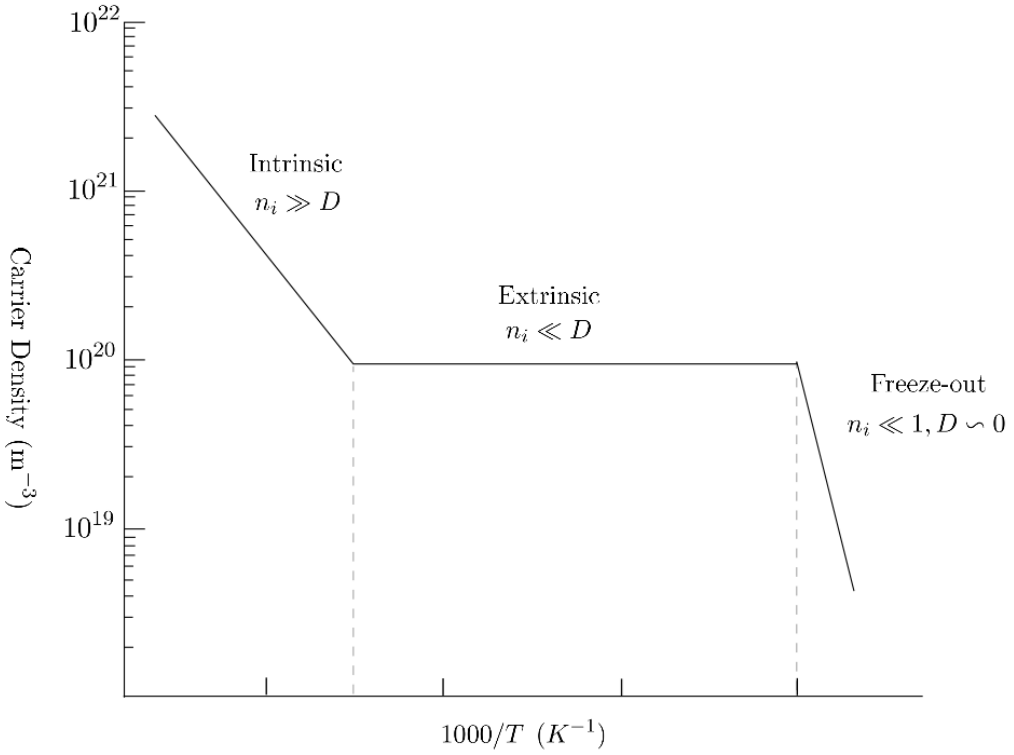

Figure 3.13: A schematic diagram of the temperature dependence of the total carrier density in semiconductors. Note the logarithmic scale on the vertical axis

4. *Magnetism*

This chapter aims to cover some of the basic concepts assocaited with magnetism, including:

- Electron Configurations
- Non-Spontaneous Magnetism
- Spontaneous Magnetism

Due to its complexity, magnetic effects still remain an active area of research in Physics. As such, the treatment of magnetism offered here is only a cursory one, but there is not much more that we can cover at an undergraduate level. We will be particularly concerned with ferromagnetic materials. Recall the following:

$$\mathbf{M} = \chi_m \mathbf{H}, \quad \mathbf{H} = \frac{B}{\mu_0} - \mathbf{M}, \quad \mu = \mu_0(1 + \chi_m)$$

It shall be assumed that readers are already familiar with the material of the B3 course.

4.1 Electron Configurations

It should be emphasised that magnetic phenomena are predominantly caused by the quantum mechanical behaviour of electrons; while the nucleus does have a magnetic moment, it smaller than the electronic magnetic moment by a factor of $\backsim m_e/m_p$, meaning that we will neglect it in our considerations. As we are dealing mostly with electrons, it is helpful to revisit some of the rules used to determine *electron configurations*, and the quantum numbers j, ℓ and s that specify the *terms* and *levels* of the system.

We already know that electronic shells should be filled by starting with the lowest energy state, and an entire shell must be filled before another is started. Furthermore, the energy ordering is from the lowest value of $(n+\ell)$ to the largest; when two shells have the same value of $(n+\ell)$, the one with the smaller n is filled first. This gives rise to the familiar ordering:

$$1s, 2s, 2p, 3s, 3p, 4s, 3s, 4p, 5s, 4d, 5p, 6s, 4f, \ldots$$

The maximum number of electrons in an orbital of a given ℓ is $2(2\ell+1)$ due to the degeneracy in both n and s. For example, neon Ne has $Z = 10$. This means that it has filled $1s, 2s$ and $2p$ shells, with the configuration Ne : $1s^2 2s^2 3p^6$. Note that it has closed outer shells.

In order to determine the terms and levels of a system, we need to invoke *Hund's rules* for the groundstate configuration of atoms. We have already met these in the B3 course, but we shall state them here in a slightly different - and more useful for our purposes - form. These are as follows:

1. Electrons try to align their spins - This is as a result of the exchange interaction; aligned spins have an antisymmetric spatial wavefunction, meaning that they are on average found further away from one another. This means that the electronic screening of the nucleus is reduced, lowering the energy of the system
2. Electrons try to maximise their total orbital angular momentum, consistent with Hund's first rule
3. Given Hund's first and second rules, the orbital and spin angular momentum either align or anti-align, so that the total angular momentum is $J = |L \pm S|$, with the sign being determined by whether the shell of orbitals is more than half filled $(+)$ or less than half filled $(-)$

Let us consider an example to gain a better understanding of how to employ these rules. For example, consider sulfur S $Z = 16$. This has electronic configuration S : $[\text{Ne}]3s^2 3p^4$. Clearly, $L = 1$ in this case. The values that M_L can take are $-1, 0, 1$. We can determine the spin states of the system using a helpful method. Write out the possible values of M_L, and then place arrows below each of these states corresponding to the spin of an electron.

$$\begin{array}{rccc} M_L = & -1, & 0, & 1 \\ & \uparrow\downarrow & \uparrow & \uparrow \end{array} \tag{4.1}$$

This is done moving left to right, placing up arrows first. If we run out of non-occupied spin states (i.e we have placed an up arrow below all values of M_L) and we still have outer-shell electrons that have not been assigned, we start again from the left, but placing down arrows this time. Then, any states with an up and a down arrow have $s = 0$, while those with a single up arrow are $s = 1/2$. The total spin S of the system is then the sum of these spins. Thus, for sulfur $S = 1$. Then, the outer shell is more than half filled, so $J = L + S = 2$. The term for sulfur in the groundstate is thus ${}^3P_2$.

4.2 Non-Spontaneous Magnetism

Non-spontaneous magnetic effects require the application of an external magnetic field. In particular, we have

- Paramagnetism - The total angular momentum J of individual atoms in a material is non-zero, meaning that they have an intrinsic magnetic moment. When an external magnetic field is applied, these magnetic moments align with the field, creating an induced magnetisation in the direction of the applied field ($\chi_m > 0$). This decreases the energy of the system. Examples include the free electron gas, free e^- metals (group I), and ferromagnets above critical temperature (more on this in section 4.3.2)
- Diamagnetism - The total angular momentum J of individual atoms is zero, meaning that all spin states are paired within the atomic structure. When an external magnetic field is applied, internal magnetic fields are created that are in the opposite direction to the applied field ($\chi_m < 0$). This increases the energy of the system. Examples include the noble gases, and inert molecules with filled outer shells (N_2).

We can derive a Hamiltonian to describe these magnetic effects. Recall the definition of the Bohr magneton

$$\boxed{\mu_B = \frac{e\hbar}{2m_e}} \tag{4.2}$$

Consider an atom of total orbital angular momentum $\mathbf{L}$ and spin angular momentum $\mathbf{S}$, in an external magnetic field described by the magnetic vector potential $\mathbf{A}$. This will have Hamiltonian

$$\begin{aligned} H &= \frac{1}{2m_e}(\mathbf{p} + e\mathbf{A})^2 + U(r) + g_s\frac{\mu_B}{\hbar}\mathbf{B}\cdot\mathbf{S} \\ &= \frac{\mathbf{p}^2}{2m_e} + U(r) + \frac{e^2}{2m_e}\mathbf{A}^2 + \frac{e}{m_e}\mathbf{p}\cdot\mathbf{A} + g_s\frac{\mu_B}{\hbar}\mathbf{B}\cdot\mathbf{S} \end{aligned} \tag{4.3}$$

where g_s is the spin g-factor. We shall consider the magnetic field to be uniform, as it is very difficult to create a field that has significant spatial variation over the largescale of the atom. This means that a convenient choice of $\mathbf{A}$ is

$$\mathbf{A} = \frac{1}{2}\mathbf{B}\times\mathbf{r} \tag{4.4}$$

Then, we can write our Hamiltonian as

$$H = H_{CF} + \frac{e}{2m_e}\mathbf{p}\cdot(\mathbf{B}\times\mathbf{r}) + g_s\frac{\mu_B}{\hbar}\mathbf{B}\cdot\mathbf{S} + \frac{e^2}{2m_e}\frac{1}{4}|\mathbf{B}\times\mathbf{r}|^2 \tag{4.5}$$

where H_{CF} is the central field Hamiltonian for an electron in the absence of an external magnetic field. We can rearrange this second term as

$$\frac{e}{2m_e}\mathbf{p}\cdot(\mathbf{B}\times\mathbf{r}) = \frac{e}{2m_e}\mathbf{B}\cdot(\mathbf{r}\times\mathbf{p}) = \frac{e}{2m_e}\mathbf{B}\cdot\mathbf{L} \tag{4.6}$$

meaning that our overall Hamiltonian cab be written as

$$\boxed{H_B = H_{CF} + \frac{\mu_B}{\hbar}(\mathbf{L} + g_s\mathbf{S})\cdot\mathbf{B} + \frac{e^2}{2m_e}\frac{1}{4}|\mathbf{B}\times\mathbf{r}|^2} \tag{4.7}$$

The second term is responsible for paramagnetism (we recognise the magnetic moment $\boldsymbol{\mu} = -(\mu_B/\hbar)(\mathbf{L} + g_s\mathbf{S})$), while the third is responsible for diamagnetic effects. For small applied magnetic fields, the diamagnetic term is much smaller than the diamagnetic term due to the quadratic dependence on $\mathbf{B}$.

4.2.1 Curie Paramagnetism

We have already examined Pauli paramagnetism in section 1.3.2. We choose to now focus on *Curie paramagnetism* (also known as free-spin paramagnetism) that is described by the Hamiltonian

$$\delta H_{\text{paramagnetic}} = \frac{\mu_B}{\hbar}(\mathbf{L} + g_s\mathbf{S}) \cdot \mathbf{B} \tag{4.8}$$

It is clear that the application of $\mathbf{B}$ lowers the energy of the system as $\mathbf{L}$ and $\mathbf{S}$ align with the field.

Free Spin 1/2

Let us consider the case of a system of N spin-half electrons with $\mathbf{L} = 0$. By (4.8), the Hamiltonian has energy eigenvalues $\pm\mu_B B$, where we have taken $g_s \approx 2$ for electrons. The single particle partition function is then

$$Z_1 = \sum_\alpha e^{-\beta E_\alpha} = e^{\beta\mu_B B} + e^{-\beta\mu_B B} = 2\cosh(\beta\mu_B B) \tag{4.9}$$

This means that the overall partition function for our system is given by

$$Z = Z_1^N = 2^N \cosh^N(\beta\mu_B B) \quad \longrightarrow \quad F = -Nk_BT\log(2\cosh(\beta\mu_B B)) \tag{4.10}$$

We now define the *magnetisation* and *magnetic susceptibility* of the system by

$$\boxed{M = -\frac{1}{V}\left(\frac{\partial F}{\partial B}\right)_T, \quad \chi_m = \lim_{H\to 0}\frac{\partial M}{\partial H}} \tag{4.11}$$

In this case, the magnetisation is clearly given by

$$M = n\mu_B \tanh\left(\frac{\mu_B B}{k_B T}\right) \tag{4.12}$$

In the weak field - or high temperature - limit, such that $\beta\mu_B B \ll 1$, we obtain an expression for the magnetic susceptibility as

$$\chi_{\text{Curie}} = \frac{n\mu_0\mu_B^2}{k_B T} \tag{4.13}$$

The dependence $\chi_m \backsim C/T$ for some constant C is known as *Curie's Law*, which we find is the case for many magnetic systems at low temperatures.

Free Spin J

In reality, the orbital angular momentum of the electrons cannot be ignored, such that we have to use the most general Hamiltonian (4.8). Without loss of generality, we choose to orient the magnetic field along $\mathbf{e}_z$. In this case, it is clear that J^2, J_z, L^2 and S^2 are all constants of the motion, meaning that we adopt the eigenstates $|J, M_J, L, S\rangle$. The change in the energy is given by first order perturbation theory as

$$\delta E_{\text{para}} = \frac{\mu_B}{\hbar} B \langle J, M_J, L, S| (L_z + 2S_z) |J, M_J, L, S\rangle = \frac{\mu_B}{\hbar} B(M_J\hbar + \langle S_z\rangle) \tag{4.14}$$

where we have used the fact that $J_z = L_z + S_z$. We can now employ a corollary of the Wigner-Eckart theorem, which states that:

$$\langle J, M_J| \mathbf{v} |J', M_J'\rangle \propto \langle J, M_J| \mathbf{J} |J', M_J'\rangle \tag{4.15}$$

That is, the expectation value of any vector operator $\mathbf{v}$ in a basis where total angular momentum is conserved (i.e that J and M_J are good quantum numbers) is proportional to the expectation value of $\mathbf{J}$ in that state. Thought of in terms of the vector model, this describes how any component perpendicular to $\mathbf{J}$ is time-averaged to zero due to procession around this axis. We thus write

$$\langle J, M_J, L, S| \mathbf{S} |J, M_J, L, S\rangle = \langle \mathbf{S} \rangle = c \langle \mathbf{J} \rangle \tag{4.16}$$

for some constant of proportionality c. Taking the dot product with $\mathbf{J}$:

$$\langle \mathbf{J} \cdot \mathbf{S} \rangle = cJ(J+1)\hbar^2 \quad \longrightarrow \quad c = \frac{\langle \mathbf{J} \cdot \mathbf{S} \rangle}{J(J+1)\hbar^2} \tag{4.17}$$

It follows that

$$\langle S_z \rangle = \frac{\langle \mathbf{J} \cdot \mathbf{S} \rangle \langle J_z \rangle}{J(J+1)\hbar^2} = \frac{M_J \langle \mathbf{J} \cdot \mathbf{S} \rangle}{J(J+1)\hbar^2} \tag{4.18}$$

We then note that

$$\mathbf{J} \cdot \mathbf{S} = \frac{1}{2}(\mathbf{J}^2 - \mathbf{L}^2 + \mathbf{S}^2) \tag{4.19}$$

such that we obtain the energy eigenvalues

$$\delta E_{\text{para}} = M_J \mu_B B \left[1 + \frac{J(J+1) - L(L+1) + S(S+1)}{2J(J+1)}\right] \tag{4.20}$$

The bracketed term is denoted g_J, known as the Landé g-factor, allowing us to write our energy levels as $M_J g_J \mu_B B$. For a single electron, we must sum over the $2J+1$ values of M_J. Defining $x = g_J \mu_B B \beta$, we can write the single particle partition function as

$$Z_1 = \sum_{M_J=-J}^{J} e^{-xM_J} = \frac{e^{-xJ} - e^{x(J+1)}}{1 - e^x} = \frac{\sinh\left[\left(J + \frac{1}{2}\right)x\right]}{\sinh\left[\frac{1}{2}x\right]} \tag{4.21}$$

If we again assume that there are N electrons in our system, the Gibbs free energy becomes

$$F = -k_B T \log\left(Z_1^N\right) = -N k_B T \left[\log\left(\sinh\left[\left(J + \frac{1}{2}\right)x\right]\right) - \log\left(\sinh\left[\frac{1}{2}x\right]\right)\right] \tag{4.22}$$

The magnetisation is then given by

$$\boxed{M = n\mu_B g_J J B_J(x), \quad B_J(x) = \frac{1}{J}\left[\left(J + \frac{1}{2}\right)\coth\left[\left(J + \frac{1}{2}\right)x\right] - \frac{1}{2}\coth\left[\frac{x}{2}\right]\right]} \tag{4.23}$$

The expression $B_J(x)$ is known as the Brillouin function, as plotted in figure 4.1. It is clear that for $x \gg 1$, $B_J \to 1$, which simply tells that all of the magnetic moments of the electrons are aligned with the external magnetic field. In reality, the energy of the magnetic interaction is usually quite weak in comparison to the thermal energy of the system, meaning that we generally consider the case of $x \ll 1$. Using the expansion $\coth y \approx y^{-1} + y/3$, we can find the magnetic susceptibility of the system as

$$\boxed{\chi_{\text{Curie}} = \frac{n\mu_0(g_J\mu_B)^2}{3}\frac{J(J+1)}{k_B T}} \tag{4.24}$$

Note that Curie law susceptibility always diverges at low temperatures. This means that if J is non-zero Curie paramagnetism dominates over other forms of magnetism.

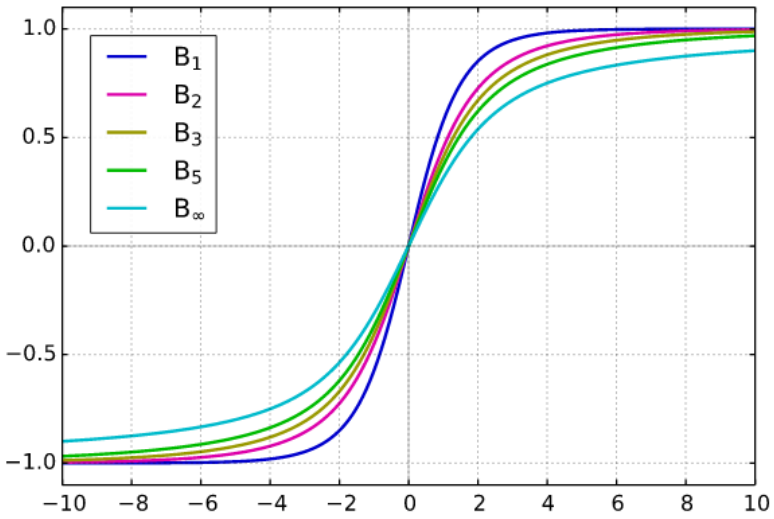

Figure 4.1: Plotting the Brillouin function $B_J(x)$ for $J = 1$, $J = 2$, $J = 3$, $J = 5$ and $J \to \infty$

4.2.2 Larmor Diamagnetism

The only time we can ever observe diamagnetic is if $J = 0$, as otherwise it is completely overshadowed by Curie paramagnetism. This often occurs in atoms with filled outer shells, such as the noble gases. Consider the diamagnetic term in (4.7):

$$\delta H_{\text{diamagnetic}} = \frac{e^2}{2m_e}\frac{1}{4}\left|\mathbf{B}\times\mathbf{r}\right|^2 \tag{4.25}$$

We again assume that $\mathbf{B}$ is orientated along $\mathbf{e}_z$, such that first order shift in the energy can be written as

$$\delta E_{\text{dia}} = \frac{e^2}{8m_e}\left\langle\left|\mathbf{B}\times\mathbf{r}\right|^2\right\rangle = \frac{e^2B^2}{8m_e}\left\langle x^2+y^2\right\rangle \tag{4.26}$$

As our atoms exhibit spherical symmetry, we can use spatial isotropy to write that

$$\left\langle x^2+y^2\right\rangle = \frac{2}{3}\left\langle x^2+y^2+z^2\right\rangle = \frac{2}{3}\left\langle r^2\right\rangle \tag{4.27}$$

such that the energy shift becomes

$$\delta E_{\text{dia}} = \frac{e^2B^2}{12m_e}\left\langle r^2\right\rangle \tag{4.28}$$

The magnetic moment m for each electron is then given by

$$m = -\frac{\partial\delta E_{\text{dia}}}{\partial B} = -\left[\frac{e^2}{6m_3}\left\langle r^2\right\rangle\right]B \tag{4.29}$$

Assuming that there is a density $\rho = Zn$ of electrons within the system, we can write the magnetic susceptibility as

$$\boxed{\chi_{\text{Larmor}} = -\frac{Zne^2\mu_0\left\langle r^2\right\rangle}{6m_e}} \tag{4.30}$$

This accounts for the diamagnetic of electrons in core orbitals. For the conduction of electrons in a metal, we need to consider the Landau-diamagnetism $\chi_{\text{Landau}} = -\chi_{\text{Pauli}}/3$ that combines with the Pauli paramagnetism to reduce the total magnetism of the conduction electrons by 1/3.

4.3 Spontaneous Magnetism

Spontaneous magnetic effects occur without the application of an external magnetic field, and usually occurs due to the coupling between electronic spins within materials. In the presence of a magnetic field $\mathbf{B}$, we can write this ineraction in the *Heisenberg Hamiltonian*

$$\boxed{H = -\frac{1}{2}\sum_{\langle i,j\rangle} J\,\mathbf{S}_i \cdot \mathbf{S}_j - \kappa \sum_i (S_i^z)^2 + g_s \mu_B \mathbf{B} \cdot \sum_i \mathbf{S}_i} \tag{4.31}$$

where $\langle i, j\rangle$ indicates a sum over neighbouring particles, and we have assumed that the coupling strength between neighbouring atoms is constant $J_{ij} = J$. We have also assumed that the system is in the groundstate, and that we are at absolute zero, meaning that we do not have to worry about thermal fluctuations causing excitations within our system. The first term describes coupling between adjacent spins, while the second is an anisotropy term that favours spins to be pointing up or down along $\mathbf{e}_z$, but not in any other direction. The last term describes the interaction of all of the spins with some external magnetic field.

Some spontaneous magnetic interactions include:

- Ferromagnetism - If $J > 0$ in (4.31), neighbouring spins tend to align. In the groundstate, this will tend to occur macroscopically, creating a net magnetic moment. Ferromagnetic materials are usually modelled using *domains* - regions where the local magnetic moments are all aligned - which re-orient themselves upon the application of a sufficiently large magnetic field. This is the origin of magnetic hysteresis, which we will study in detail in the next section

- Anti-ferromagnetism - If $J < 0$, neighbouring spins will tend to oppose one another, and so the minimum energy state occurs when they alternate. This means that there is no net magnetic moment, but the spins are internally ordered due to magnetic effects

- Ferrimagnetism - These are antiferromagnets ($J < 0$) that have a net magnetic moment due to the fact that they contain more than one type of atom in the unit cell, which means that they all have different magnetic moments which do not cancel. In this case, we need to include the anisotropy term in (4.31)

- Itinerant ferromagnetism - This is similar to ferromagnetism, except the spins involved are not localised within the material, meaning that the aligned spins can wander throughout the system. Unlike the other magnetic effects above, this is described by the *Hubbard Hamiltonian*

$$H = H_0 + \sum_i U n_{i\uparrow} n_{i\downarrow} \tag{4.32}$$

  where H_0 includes the kinetic energy of the system, while the second term encodes the interactions between spins. U parametrises the repulsive Hubbard interaction energy, while $n_{i\uparrow}$ and $n_{i\downarrow}$ denote the number of electrons at site i with spin-up and spin-down respectively

Though magnetism can be interesting, it can also get quite complicated. For this reason, we shall only examine ferromagnetic effects in further detail in this text; the other magnetic effects can be left to the independent investigation of the reader.

4.3.1 Domains and Hysteresis

As previously stated, *domains* are regions of a ferromagnet in which all the spins are locally aligned. The competition between local spins lining up and regional dipoles give rise to domain boundaries. Even though some opposite spins close to the boundaries will not be aligned, there is a global energy saving for the entire system to organise itself in a domain structure.

The precise nature of this structure depends very specifically on, for example, the ratio of the long-range to short-range spin coupling interactions within the material. In some cases, the positions of the domain walls can be influenced by defects in the crystal. If an atom is missing along a domain wall, there are fewer opposite spins next to one another, which is an energetically preferable state. This means that the domain wall will often stay *pinned* to the defect even when the domains shift.

There are many different types of domain walls that can occur, given the potentially complicated lattice structure of the material. In many cases, it is preferable to assume that the spins either point up or down along some direction, meaning that the anisotropy term κ is very large. This leads to an infinitely 'sharp' domain wall. The *Bloch wall* is includes a smooth transition between spin-up and spin-down states over some lengthscale ℓ, as depicted in figure 4.2 below.

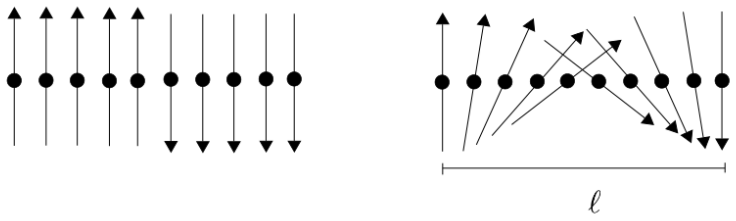

Figure 4.2: An infinite domain wall (left) and a Bloch wall (right)

The lengthscale of the domain wall ℓ will clearly depend on a balance between the coupling J and the anisotropy κ; if κ/J is large, the spins want to point in opposite directions, but if κ/J is small, it costs little energy to point spins in other directions. Let us estimate this lengthscale ℓ.

Assume that the length of the wall is $\ell = Na$, for the lattice constant a. If we assume the twist angle is constant, it will twist an amount $\delta\theta = \pi/N$ each time. The energy associated with a single spin-spin interaction is approximately

$$E_{ij} = -J\mathbf{S}_i \cdot \mathbf{S}_j = -JS^2 \cos(\theta_i - \theta_j) \approx -JS^2 \left(1 - \frac{(\delta\theta)^2}{2} + \dots\right) \tag{4.33}$$

This means that the energy penalty for these spins not being aligned is

$$\delta E_{ij} = JS^2 \frac{(\delta\theta)^2}{2} = JS^2 \frac{\pi^2}{2N^2} \tag{4.34}$$

This means that the energy penalty of the spins not being aligned (sometimes called *stiffness*) per unit area A of the domain wall is given by

$$\frac{\delta E_{ij}}{A/a^2} = NJS^2 \frac{\pi^2}{2N^2} \tag{4.35}$$

where we have expressed A in units of the lattice constant a. We can approximate the energy penalty due to the anisotropy term as being approximately κS^2 per spin, such that

$$\frac{\delta E_\kappa}{A/a^2} \approx \kappa S^2 N \tag{4.36}$$

This means that total energy of the Bloch domain wall can be written as

$$\boxed{\frac{E_{\text{wall}}}{A/a^2} = \frac{\pi^2}{2} J S^2 \left(\frac{1}{N} + \frac{2\kappa}{\pi^2 J} N \right)} \tag{4.37}$$

where we have expressed A in units of a. If we assume that E_{wall} is constant, this can be minimised to give $N \backsim (J/\kappa)^{1/2}$, meaning that ℓ scales as the square-root of the ratio $J\kappa$. Evidently, the domain wall costs energy, but this is outweighed in most cases by the long range dipolar effects.

Hysteresis

The application of an external magnetic field to domains causes them to shift, and align with the external magnetic field. When this external field is turned off, there will be some residual magnetisation. In short, this is because there is a large activation energy in order to re-orient the domains, as we shall now show.

Consider the energy per unit volume of some small crystallite within the material that has magnetisation $\mathbf{M}$. Motivated by (4.31), we can write its energy per unit volume as

$$E/V = E_0 - \mathbf{M} \cdot \mathbf{B} - \bar{\kappa} (M^z)^2 \tag{4.38}$$

where we have orientated the crystal axis along $\mathbf{e}_z$. E_0 is some constant energy term arising from the fact that we assume that all of the moments within the crystallite are aligned with one another, while $\bar{\kappa}$ is related to the original anisotropy term κ. Assume that the magnetic field $\mathbf{B}$ is also orientated along $\mathbf{e}_z$, such that

$$E/V = E_0 - |\mathbf{M}||\mathbf{B}| \cos\theta - \bar{\kappa} |\mathbf{M}|^2 \cos^2\theta \tag{4.39}$$

where θ is the angle between $\mathbf{M}$ and $\mathbf{e}_z$. This is a parabola in the variable $\cos\theta$. Evidently, the minimum is at $\theta = 0$, when the magnetisation is aligned with the external field. However, a local minimum also exists for $|\mathbf{B}| < B_c = 2\bar{\kappa}|\mathbf{M}|$ where the spins are aligned in the opposite direction to the external field $\theta = \pi$.

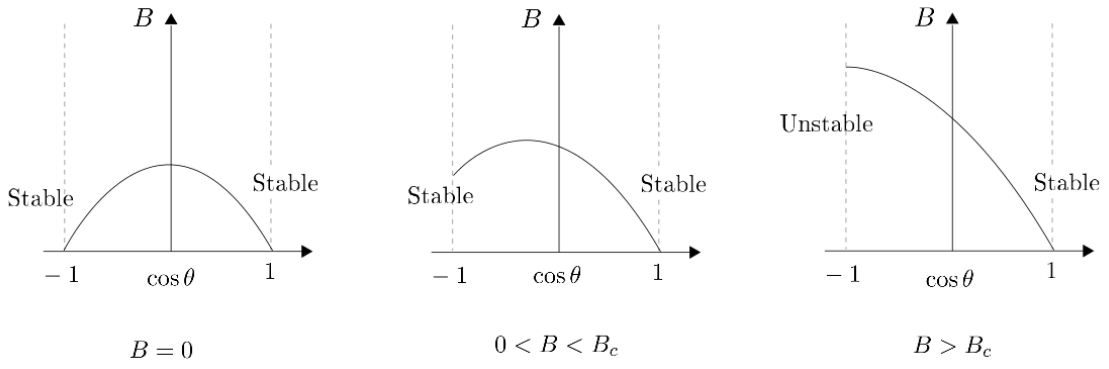

Figure 4.3: The solution to (4.39) for different values of B

This can explain hysteresis behaviour; a certain field field must be applied to these crystallites before they can re-orient themselves. In the case of domains and domain walls, there might be some activation energy that is required to shift them at all (higher for pinned domains), meaning that an applied magnetic field is required to return the magnetisation to zero. Many permanent magnets have artificially pinned domain walls such that a large energy barrier must be overcome in order to demagnetise them.

A useful way of representing these processes is using a *hysteresis curve* that is shown in figure 4.4.

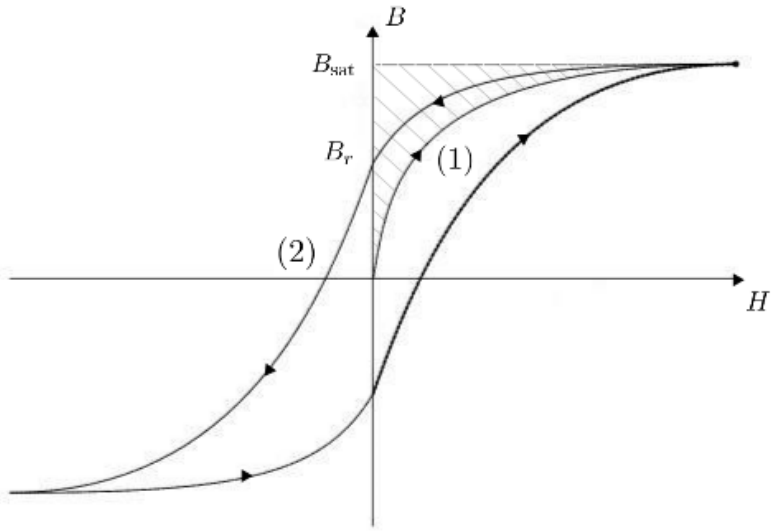

Figure 4.4: An example hysteresis curve

Some key features of this to note:

- Magnetisation curve (1) - The response of the material under the applied field when it is initially unmagnetised
- Coercive force (2) - The strength of the applied field required to demagnetise the material
- Magnetisation energy - The shaded area gives the energy required to magnetise the material. More generally, the work done to move around a closed loop in this plane is given by

$$W = \oint d\mathbf{B} \cdot \mathbf{H} \tag{4.40}$$

- Saturation field B_{sat} - The strength of the magnetic field at saturation (when all the domains are aligned)
- Remnant field B_r - The field that remains when the applied field has been reduced to zero

Generally, materials that have a narrow hysteresis curve are called *soft*, while those with a wide curve are called *hard*; it takes less energy to go around a soft curve than a hard one, meaning that it is easier to change the magnetisation of soft materials.

4.3.2 Weiss Molecular Field Theory

The simplest model of ferromagnetism is to adopt a mean-field theory, in which we examine determine the behaviour of one atomic site exactly, and then insist that all small regions should look the same such that the model remains self-consistent. Consider (4.31) for $\kappa = 0$:

$$H = -\frac{1}{2}\sum_{\langle i,j\rangle} J\,\mathbf{S}_i \cdot \mathbf{S}_j + g_s\mu_B \mathbf{B} \cdot \sum_i \mathbf{S}_i \tag{4.41}$$

For a single site i, we write that

$$H_i = \left[g_s\mu_B \mathbf{B} - J\sum_j \mathbf{S}_j \right] \cdot \mathbf{S}_i \tag{4.42}$$

where the sum runs over the nearest neighbours j of i. This can be re-formulated as

$$H_i = g_s\mu_B \langle B_{\text{eff}}\rangle S_i, \quad B_{\text{eff}} = B - \frac{J}{g_s\mu_B}\sum_j S_j \tag{4.43}$$

This Hamiltonian has eigenvalues $E_i = \pm g_s\mu_B \langle B_{\text{eff}}\rangle /2$, meaning that it is easy to show that the Gibbs free energy is given by

$$F = -k_B T \log\left[2\cosh\left(\frac{1}{2} g_s\mu_B\beta \langle B_{\text{eff}}\rangle\right)\right] \tag{4.44}$$

Then, the expectation value of the spin state from site i is given by

$$\langle S_i\rangle = \frac{\partial F}{\partial \langle g_s\mu_B B_{\text{eff}}\rangle} = -\frac{1}{2}\tanh\left(\frac{1}{2} g_s\mu_B\beta \langle B_{\text{eff}}\rangle\right) \tag{4.45}$$

However, we have that

$$\langle B_{\text{eff}}\rangle = B - \frac{J}{g_s\mu_B}\sum_j \langle S_j\rangle = B - \frac{J}{g_s\mu_B} z \langle S_i\rangle \tag{4.46}$$

The last expression follows from the assumption that all neighbouring lattice sites experienced the same magnetic field, such that we can $\langle S_j\rangle = \langle S_i\rangle$. Note that z is the coordination number that we met in section 2.1.2. Letting $\langle S_i\rangle \equiv \langle S\rangle$, we can write that

$$\boxed{\langle S\rangle = -\frac{1}{2}\tanh\left[\frac{1}{2}\beta\left(g_s\mu_B B - Jz\langle S\rangle\right)\right]} \tag{4.47}$$

This is an implicit equation for $\langle S\rangle$, the expectation value of the spin for a given site within the system. Evidently, this cannot be solved analytically. Instead, let us look for a graphical solution for the case that $B = 0$, where

$$\langle S\rangle = \frac{1}{2}\tanh\left[\frac{1}{2}\beta J z \langle S\rangle\right] \tag{4.48}$$

Plotting the left-hand side and right-hand side on the same axes will yield either one (trivial) solution (at high temperatures, corresponding to no overall magnetisation or spin), or three solutions (at low temperatures, after which the system becomes ferromagnetic). The transition between these two behaviours occurs at the *Curie temperature* T_c. This can be found by expanding $\tanh x \approx x$, such that we define

$$\boxed{k_B T_c = \frac{Jz}{4}} \tag{4.49}$$

Curie-Weiss Susceptibility

We shall consider the small magnetic field limit $\beta\mu_B B \ll 1$, such that we can also consider the induced spins to be small $\beta\langle S\rangle \ll 1$. Equivalently, this is the high temperature limit. Again expanding $\tanh x \approx x$ in (4.47), it is easy to show that

$$\langle S\rangle = -\frac{1}{4}\frac{g_s\mu_B B}{k_B T\,(1 - T_c/T)} \tag{4.50}$$

If V_{uc} is the volume of the unit cell, the magnetisation is given by

$$M = \frac{m}{V_{\text{uc}}} = -\frac{g_s\mu_B}{V_{\text{uc}}}\langle S\rangle \tag{4.51}$$

such that the magnetic susceptibility becomes

$$\chi_m = \frac{\mu_0(g_s\mu_B)^2}{4V_{\text{uc}}k_B T}\frac{1}{(1 - T_c/T)} \tag{4.52}$$

Thus, for n spins/sites per unit volume, the magnetic susceptibility is given by

$$\boxed{\chi_{\text{Weiss}} = \frac{n\mu_0(g_s\mu_B)^2}{4k_B T}\frac{1}{(1 - T_c/T)}, \quad T_c = \frac{Jz}{4k_B}} \tag{4.53}$$

Comparing this with (4.13), we can also write that

$$\chi_{\text{Weiss}} = \frac{\chi_{\text{Curie}}}{1 - T_c/T} \tag{4.54}$$

This is know as the *Curie-Weiss law*. From this, we can state the following key characteristics of our system as described by Weiss molecular field theory:

- There is a finite temperature phase transition from a low temperature ferromagnetic phase to a high temperature paramagnetic phase at a transition temperature known as the Curie temperature
- Above the Curie temperature, the paramagnetic susceptibility is $\chi_{\text{para}} = \chi_0/(1 - T_c/T)$, where χ_0 is the susceptibility of the corresponding model where the ferromagnetic coupling between sites is turned off (such as free spins)
- Below the Curie temperature, the magnetic moment turns on, and increases to saturation at temperatures approaching absolute zero

Note that we can apply this mean field technique to other magnetic systems in order to find their behaviour. The case of anti-ferromagnets follows trivially from this result, simply involving changing the sign of J.